7. THE PALEOMAGNETISM OF SEDIMENTS ACQUIRED FROM THE GOBAN SPUR ON DEEP SEA DRILLING PROJECT LEG 80[1]

Hilary A. Townsend, Oceanography Department, Southampton University[2]

ABSTRACT

Paleomagnetic results from sediments acquired from the continental margin at DSDP Sites 548, 549, 550, and 551 are described. Where possible, the results were used to construct a polarity reversal stratigraphy for the sections sampled, thus enabling the biostratigraphic dating of the sediments to be refined. Several sections in this study were found to be suitable for magnetostratigraphic work, in particular the upper Paleocene to middle Eocene sediments from Site 549, which contained rich faunal assemblages. These sediments are underlain by a thick sequence of Cretaceous sediments that formed during the Long Cretaceous normal polarity interval. Sediments that formed during the later part of this magnetically quiet interval were also recovered at Site 550. Three short reverse polarity intervals were also recovered at this site; they lie directly over basement and are thought to represent a mixed-polarity interval of late Albian age. They may therefore provide important evidence concerning the age of the earliest sediments at this site.

In addition, measurements of the magnetic susceptibility and intensity of remanent magnetism proved to be of interest. A significant decrease in the susceptibility and intensity values close to the early/middle Eocene boundary was noted at Sites 548 and 549. This decrease may be correlated with the results from Holes 400A and 401, which were drilled on DSDP Leg 48 in the northeast Bay of Biscay. The decrease may represent an abrupt reduction in the supply of terrigenous material at the end of the early Eocene, reflecting, perhaps, a change in sediment transport processes at that time.

INTRODUCTION

This paper describes the results of paleomagnetic studies carried out on the sediments recovered from four sites drilled along a transect across the northern Biscay continental margin during Leg 80 of the Deep Sea Drilling Project. The main aim of this study was to construct a magnetic stratigraphy that would complement the biostratigraphic studies and provide additional information on the geological ages of the sediments drilled and the dating of the major paleoceanographic events recorded in the sediments.

PALEOMAGNETIC TECHNIQUES

Sampling Procedures

Paleomagnetic samples were taken from the relatively soft sediments by using 2.5-cm plastic cylinders that were then sealed with cellophane to prevent the sediment from drying out. In the case of the consolidated sediments, 2.5-cm-diameter cylinders were drilled with a diamond-tipped core drill. In both cases an uphole orientation line was carefully marked on the samples before they were removed from the core.

Measuring Procedures

Most of the measurements of direction and intensity of remanence were carried out on a standard Digico spinner magnetometer (Molyneux, 1971) installed on the *Glomar Challenger.* The samples were incrementally demagnetized in an alternating field (af) by using a Schonstedt single-axis demagnetizer. Subsequent measurements were completed after the cruise in the paleomagnetic laboratory at Southampton University. Throughout the period of the cruise the average noise level of the shipboard magnetometer was 0.05 μG.

At Sites 548 and 549 the variable length hydraulic piston corer (VLHPC) was used for the first time; a method for orienting the cores was also tested at these two sites. Knowledge of the orientation of a core would permit the absolute azimuth of the core to be measured so that the assignment of polarity could be based on both the declination and the inclination of stable remanent magnetization rather than inclination only. Unfortunately, as a result of technical difficulties fewer than half the cores could be oriented at these sites, so the new facility was of limited value on Leg 80. However, the additional paleomagnetic information available from having oriented IPOD cores should prove to be useful in the future.

Figure 1 shows the stratigraphic variation of declination and inclination for the upper 80 m at Site 548, where the absolute azimuth was successfully recorded in a number of cores. After magnetic cleaning, the oriented cores generally possessed a northerly paleomagnetic declination (360 ± 20°) and a positive inclination, characteristics indicative of a normal polarity stable direction. A single oriented sample at 72 m yielded a shallow negative inclination and a more southerly declination, which suggests that a short magnetic event occurred at this point in the Brunhes normal polarity epoch.

Figure 1 shows one of only a few short intervals where the azimuth of the core was recorded successfully, however. In most of this study the assignment of the magnetic polarity is based on the variation in the inclination

[1] Graciansky, P. C. de, Poag, C. W., et al., *Init. Repts. DSDP*, 80: Washington (U.S. Govt. Printing Office).

[2] Address: Oceanography Department, Southampton Unviersity, SO9 5NH, United Kingdom.

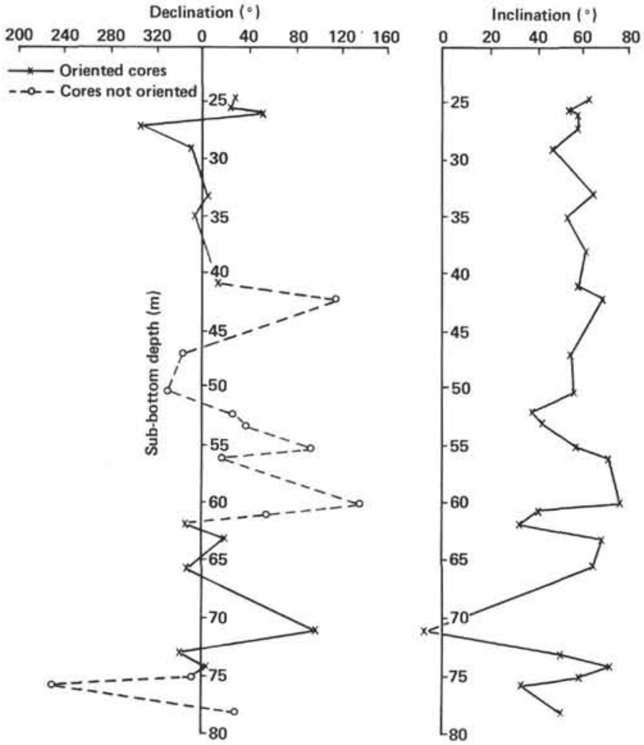

Figure 1. Downhole variation of declination and inclination at Hole 548.

of the stable remanent magnetization alone. Since the sites are situated in the Northern Hemisphere, positive inclinations are taken to signify normal polarity and negative inclinations reverse polarity.

RESULTS

Site 548

Site 548, which was the shallowest site in the Goban Spur transect, was drilled on the seaward edge of a tilted block of Hercynian basement. Two holes were drilled at this site, Hole 548 with the VLHPC and Hole 548A with the conventional rotary drill.

Hole 548

Recovery from Hole 548 was extremely good, and approximately 200 oriented samples from the Pleistocene and Pliocene sediments were taken. Each sample was demagnetized in an alternating field until the polarity of the stable component was considered unequivocal. The more strongly magnetized samples were demagnetized at peak fields up to 200 or 300 Oe; the intensity of the more weakly magnetized samples became too weak for reliable measurement after demagnetization at fields greater than 75 or 100 Oe. The results from this hole are summarized in Table 1. Figure 2 illustrates the behavior of four samples from this hole on demagnetization. Two of the samples (548-10-4, 6-8 cm and 548-1-1, 14-43 cm) are moderately stable and have been assigned a normal polarity. The other two are reverse polarity samples. One of them (Sample 548-10-5, 6-8 cm) has a reasonably high stability, whereas the other (Sample 548-10-5, 84-86 cm) has a shallow initial negative inclination that becomes steeper on demagnetization, suggesting that a secondary component is being removed during the demagnetization process.

Magnetic Polarity Record

Figure 3 shows the stratigraphic variation of magnetic inclination after optimum demagnetization, together with the inferred polarity reversal sequence and the assigned anomaly numbers. The biostratigraphic zones established (Müller, this volume and Snyder, this volume) have also been included in the figure. In the upper section there is a long normal polarity interval (down to 84 m sub-bottom) that contains evidence of a possible magnetic field excursion. Below this interval there are two well-defined normal polarity intervals that are thought to represent the Jaramillo and Olduvai events. The Olduvai Event spans the Pleistocene/Pliocene boundary, which has been placed at approximately 102 m sub-bottom on nannofossil evidence (Müller, this volume). In the Pliocene sediments a further sequence of polarity reversals is evident. They are not as well defined as the later reversals, but they probably correspond to the sequence of polarity changes that together represent Anomalies 2A and 3.

NRM Intensity and Volume Susceptibility

Figure 4 shows the downhole variation of NRM intensity and volume susceptibility. The correlation of the two plots is good, suggesting that the NRM intensity reflects magnetic mineral content instead of variations in the intensity of the geomagnetic field at the time of deposition. The abrupt decrease in intensity and susceptibility at approximately 59 m sub-bottom corresponds to the lithologic change between Subunits 1a and 1b, which is distinguished by a downward decrease in terrigenous material and an increase in calcium carbonate. The minor fluctuations in NRM intensity and volume susceptibility also seem to correspond to small variations in the amount of marly material.

Hole 548A

Approximately 220 samples were taken from Hole 548A, and the paleomagnetic results are summarized in Table 2. The results from the upper part of the hole (down to 380 m sub-bottom) are difficult to interpret because the sequence is condensed in parts. In addition, the frequency of magnetic field reversals was relatively high during the Miocene and Oligocene epochs. Inasmuch as the sediments from this section are also very weakly magnetized (0.03-0.20 μG), no conclusive magnetic polarity reversal sequence can be defined.

The samples below 380 m sub-bottom have considerably higher NRM intensities (0.20-50.0 μG), and most were demagnetized in peak fields up to 200 or 300 Oe. Figure 5 illustrates the behavior of a typical normal polarity sample (548A-33-2, 107-109 cm) and a reverse polarity sample (548A-33-1, 106-108 cm). The magnetization direction of the normal polarity sample is moderately stable; the reverse polarity sample shows a considerable change between the NRM and 100 Oe steps but little

Table 1. Paleomagnetic results, Hole 548.

Core-Section (interval in cm)	Sub-bottom depth (m)	Before demagnetization D (°)	Before demagnetization I (°)	Before demagnetization Int (μG)	Demagnetization field (Oe)	After demagnetization D (°)	After demagnetization I (°)	After demagnetization Int (μG)	Polarity
1-1, 41–43	0.41	108.0	64.3	27.82	300	120.6	62.1	15.31	N
1-2, 106–108	2.56	85.1	64.0	12.88	300	122.5	51.9	5.27	N
2-1, 57–59	4.57	338.9	55.0	12.52	200	330.9	59.3	8.43	N
2-2, 122–124	6.72	23.5	47.2	6.02	200	22.0	55.8	2.22	N
2-3, 82–84	7.82	172.5	83.0	11.11	200	181.9	65.0	3.04	N
2-4, 82–84	9.32	320.0	56.2	13.56	200	297.5	63.4	6.51	N
2-5, 19–21	10.19	163.2	62.2	22.53	200	157.5	57.0	15.39	N
2-6, 27–29	11.79	263.9	79.7	21.75	200	228.4	71.8	14.83	N
2-7, 20–22	13.20	311.0	72.7	20.74	200	284.5	70.7	13.66	N
3-1, 23–25	13.73	108.1	56.3	10.52	200	116.1	60.6	4.75	N
3-2, 45–47	15.47	330.5	57.2	18.26	200	217.5	58.2	13.17	N
3-3, 112–114	17.62	208.2	60.7	11.69	200	209.5	56.9	9.94	N
3-4, 37–39	18.37	40.4	70.4	12.02	200	45.5	76.1	8.75	N
3-5, 25–27	19.75	56.6	54.9	16.06	200	61.6	58.8	10.49	N
3-6, 35–5	21.35	10.9	64.6	10.83	200	16.7	65.7	7.39	N
3-7, 25–27	22.75	215.1	65.0	10.26	200	211.0	53.1	6.48	N
4-1, 103–104	24.02	9.2	64.7	18.21	200	26.4	61.3	14.29	N
4-2, 103–105	25.53	2.7	66.8	10.65	200	25.9	54.1	3.97	N
4-3, 48–50	26.48	39.0	64.4	19.72	200	54.7	58.3	14.52	N
4-4, 49–51	27.99	301.6	59.6	29.68	200	302.5	57.8	18.00	N
4-5, 49–51	29.49	338.5	50.7	21.27	200	349.8	48.4	13.62	N
4-6, 39–41	30.89	12.9	−82.6	25.34	200	73.1	−77.8	16.15	R
5-1, 117–119	33.67	327.3	66.0	20.84	200	1.4	66.5	11.85	N
5-3, 38–40	35.88	343.3	57.5	24.41	200	354.7	54.5	16.58	N
5-5, 36–38	38.86	341.7	59.2	15.39	200	3.8	61.6	11.41	N
5-7, 33–35	41.83	8.8	57.4	16.45	200	12.9	57.7	12.53	N
6-2, 43–45	42.43	124.3	79.7	22.19	200	114.1	69.4	13.30	N
6-4, 109–111	47.59	341.6	55.6	18.97	200	341.4	56.5	13.28	N
6-6, 107–109	50.57	330.3	55.8	18.41	200	333.0	58.9	14.7	N
7-1, 95–97	52.45	359	42.7	14.86	200	35.8	38.4	12.39	N
7-2, 18–20	53.18	42.3	59.3	11.26	200	49.6	43.2	9.48	N
7-3, 102–104	55.52	82.9	72.2	9.04	200	94.7	59.8	7.76	N
7-4, 15–17	56.15	359.9	77.1	23.09	200	16.1	73.1	11.39	N
7-6, 120–122	60.20	252.5	87.6	0.09	50	139.3	79.0	0.115	N
7-7. 30–32	60.80	27.5	54.7	0.61	50	56.5	45.5	0.95	N
8-1, 50–52	61.50	355.5	40.8	0.58	50	346.5	36.5	1.19	N
8-2, 51–53	63.01	18.4	74.7	0.76	75	23.5	73.3	0.56	N
8-3, 50–52	64.50	180.2	67.1	1.38	100	156.9	68.6	1.34	N
8-4, 50–52	66.0	327.4	78.3	8.836	100	347.5	66.6	0.63	N
8-6, 31–33	68.81	109.6	49.6	0.49	100	127.0	61.1	0.12	N
9-1, 98–100	71.48	99.9	−9.0	0.35	150	169.7	8.0	0.29	?
9-3, 29–31	73.29	305.5	65.2	0.30	100	340.5	52.3	0.16	N
10-2, 103–105		211.5	67.8	4.30	200	7.3	72.7	2.38	N
10-3, 103–105		348.0	58.6	10.07	200	349.5	58.5	8.45	N
10-4, 6–8	75.06	269.3	59.4	5.55	200	279.1	76.2	3.106	N
10-4, 84–86	75.84	254.8	37.1	4.18	300	223.2	4.3	2.23	R?
10-5, 6–8	76.56	31.6	−75.2	7.522	200	67.8	−71.7	6.48	R
10-5, 84–86	77.34	329.7	−14.6	1.24	200	326.6	−79.4	1.17	R
10-6, 6–8	78.06	54.4	71.1	1.90	200	48.1	61.7	1.07	N
10-6, 84–86	78.84	10.1	51.7	0.363	50	33.1	17.9	0.19	N?
11-1, 33–36	80.33	337.9	38.1	0.19	150	303.0	40.6	0.18	N
11-1, 101–103	81.01	306.7	−13.9	0.23	150	309.1	1.0	0.07	N?
11-3, 101–103	84.1	211.5	82.5	5.32	200	225.1	48.5	1.77	N
11-4, 33–36	84.83	227.4	24.7	1.61	200	249.7	−30.7	0.94	R
11-4, 101–103	85.51	305.2	−12.0	0.35	150	312.9	−19.2	0.35	R
11-5, 33–36	86.33	241.0	26.7	0.23	150	105.4	−5.8	0.06	R?
11-5, 101–103	87.01	237.6	−47.1	0.35	50	271.3	−35.7	0.03	R
11-6, 33–36	87.33	250.0	16.7	0.14	100	328.1	−41.2	0.09	R?
12-1, 138–140	90.88	65.1	68.9	0.44	200	221.6	38.5	0.12	N
13-1, 112–114	93.12	253.4	7.8	0.16	50	1.7	33.0	0.13	N
13-2, 106–108	94.56	187.9	30.2	0.23	150	140.2	5.1	0.17	N?
13-2, 116–118	94.66	282.2	62.3	0.16	35	224.5	81.4	0.16	N
13-3, 16–18	95.16	310.5	0.3	0.30	50	317.5	−3.7	0.12	R?
13-3, 97–99	95.97	116.2	2.0	0.33	150	154.5	−14.1	0.41	R
13-4, 16–18	96.66	258.1	34.1	0.07	100	320.4	−19.8	0.07	R
13-4, 112–114	97.62	154.6	−19.7	−.19	150	128.8	−35.8	0.32	R
13-5, 16–18	95.16	261.8	−3.2	0.52	150	267.5	−15.8	0.15	R
13-5, 106–110	99.08	245.2	−19.2	0.16	150	157.8	−9.6	0.12	R
13-5, 112–114	99.12	279.3	32.4	0.41	100	333.1	49.1	0.06	N
13-6, 16–18	99.66	215.8	35.2	0.31	150	233.0	−35.7	0.13	R
15-1, 110–112	101.1	357.9	34.2	0.13	100	357.4	20.6	0.20	N
15-2, 12–14	101.62	295.4	51.8	0.24	150	300.4	47.0	0.10	N
15-4, 12–14	104.62	253.8	13.4	0.26	150	259.5	−3.7	0.23	R?
15-4, 110–112	105.73	301.2	60.7	0.37	100	353.1	69.5	0.36	N
15-5, 110–112	107.10	118.4	71.7	0.39	100	98.7	63.2	0.40	N
15-6, 12–14	107.62	227.8	22.1	0.31	50	207.1	16.9	0.05	N?
15-7, 12–14	109.12	284.8	−4.7	0.29	100	185.3	−54.5	0.16	R
16-1, 110–112	109.60	204.4	10.4	0.09	50	120.2	20.2	0.06	?
16-2, 110–112	111.10	267.8	72.3	0.10	100	290.0	84.8	0.07	R
16-4, 110–112	112.60	285.2	−27.9	0.13	50	279.4	−28.8	0.07	R
16-4, 110–112	114.10	286.0	33.3	0.16	50	338.8	21.0	0.12	N
16-6, 28–30	126.28	22.7	43.6	0.23	50	338.8	21.0	0.12	N
19-1, 61–64	131.61	171.1	62.9	0.01	NRM				N?
19-2, 29–31	132.79	274.2	−15.8	0.06	NRM				R?
19-3, 30–33	134.3	264.3	41.0	0.38	50	275.9	50.9	0.28	N
19-4, 6–9	135.56	272.1	72.1	0.26	50	270.9	58.9	0.12	N
20-1, 23–25	136.23	124.6	79.2	0.25	50	210.7	78.1	0.11	N
20-2, 23–25	137.73	158.1	55.7	0.19	50	76.1	53.3	0.22	N?
21-1, 42–44	142.92	286.7	30.7	0.23	50	248.7	61.3	0.21	N
21-3, 45–47	144.45	253.7	21.9	0.24	50	271.9	21.9	0.20	N

Table 1. (Continued).

Core-Section (interval in cm)	Sub-bottom depth (m)	Before demagnetization			Demagnetization field (Oe)	After demagnetization			
		D (°)	I (°)	Int (μG)		D (°)	I (°)	Int (μG)	Polarity
22-1, 95-97	146.95	223.5	80.7	0.18	50	172.4	49.5	0.12	N?
22-2, 32-35	147.82	284.1	40.1	0.17	50	260.1	66.4	0.14	N
22-3, 32-35	149.32	332.9	38.3	0.13	50	343.4	27.3	0.50	N
24-1, 108-110	157.08	292.0	48.9	0.04	NRM				N?
24-2, 108-110	158.58	236.6	9.3	0.09	25	243.7	61.0	0.15	N
24-3, 49-51	159.49	341.0	54.9	0.09	NRM				N
25-1, 31-33	156.31	250.2	17.9	0.16	25	239.3	61.3	0.07	N
25-2, 31-33	157.81	241.9	49.1	0.34	50	274.4	26.2	0.16	N
25-3, 31-33	159.31	238.8	37.7	0.17	50	222.7	50.1	0.11	N
25-1, 46-48	161.46	279.5	46.8	0.09	50	259.7	16.9	0.17	N
26-3, 19-21	164.19	215.0	22.6	0.17	50	61.4	64.4	0.11	N
26-4, 19-21	165.69	267.1	−12.9	0.08	25	282.1	−23.8	0.02	R
27-1, 123-125	172.23	329.5	23.9	0.03	NRM				N?
27-2, 123-125	173.73	52.1	11.7	0.007	NRM				N?
27-3, 123-125	175.23	120.5	67.0	0.04	NRM				N?
27-4, 14-16	175.63	151.1	−13.9	0.018	NRM				R?
28-1, 40-43	176.4	258.8	56.9	0.22	50	157.6	11.2	0.09	N?
28-2, 40-43	177.90	234.5	72.6	0.10	25	159.3	57.0	0.17	N?
28-2, 110-112	178.6	170.6	46.7	0.08	25	155.0	62.0	0.06	N
28-3, 41-43	179.41	170.2	−21.2	0.26	25	161.6	−46.7	0.19	R
28-3, 95-98	179.95	92.1	6.3	0.08	25	114.9	29.6	0.04	N
28-4, 20-23	180.7	251.6	14.7	0.07	25	275.6	63.1	0.05	N
29-1, 26-29	181.29	203.7	45.0	0.14	100	200.2	−31.1	0.07	R?
29-1, 119-121	182.19	265.9	−5.0	0.03	NRM				R?
29-2, 33-35	182.83	256.2	44.2	0.26	150	350.0	−8.2	0.04	R?
29-2, 118-120	183.68	275.8	6.9	0.15	25	264.1	17.5	0.10	?
29-3, 27-29	184.27	223.8	33.8	0.16	100	245.4	0.2	0.06	R??
29-3, 118-120	185.18	336.2	−32.6	0.07	NRM				R?
29-4, 26-28	185.76	305.6	46.9	0.14	75	18.6	45.2	0.07	N
30-1, 33-35	186.35	264.1	8.5	0.06	NRM				?
30-1, 123-125	187.23	175.1	37.2	0.13	25	11.7	75.7	0.12	N
30-2, 30-32	187.80	192.7	2.5	0.02	NRM				?
30-2, 118-120	188.68	299.8	40.7	0.54	50	55.8	62.8	0.26	N
30-3, 30-32	189.30	104.0	19.3	0.02	NRM				?
30-3, 126-128	190.26	339.2	43.5	0.11	50	210.8	69.4	0.11	N?
30-4, 22-24	190.72	225.8	30.4	0.08	NRM				N?
31-1, 13-15	191.13	328.4	58.2	0.21	50	281.9	70.7	0.25	N
31-1, 129-131	192.29	268.4	−2.6	0.32	100	278.1	−2.6	0.11	R?
31-2, 13-15	192.63	170.9	40.5	0.76	50	175.8	37.6	0.61	N
31-2, 125-127	913.75	250.2	68.7	0.02	NRM				N?
31-3, 117-119	195.17	315.5	52.3	0.10	50	72.0	26.2	0.10	N?
32-1, 38-40	196.38	191.4	−30.8	0.12	25	139.5	−15.5	0.14	R
32-1, 105-108	197.03	256.0	35.6	0.17	50	224.8	51.8	0.03	N
32-2, 34-36	197.84	267.5	36.4	0.14	25	27.7	−9.5	0.07	R?
32-2, 102-104	198.52	137.3	20.0	0.05	NRM				N
32-3, 34-36	199.34	285.3	14.6	0.36	50	289.7	37.5	0.24	N
32-3, 104-106	200.4	183.4	72.8	0.09	NRM				N?
33-1, 48-50	201.48	294.2	11.1	0.021	NRM				N?
33-1, 104-106	202.04	275.7	45.3	0.07	NRM				N?
33-2, 45-47	202.95	272.4	44.5	0.06	NRM				N?
33-2, 109-111	203.59	293.8	46.0	0.12	50	187.8	53.3	0.20	N
33-3, 41-43	204.41	271.0	17.2	0.09	NRM				N?
33-3, 120-122	205.20	82.1	56.3	0.11	NRM				N
34-2, 46-48	207.96	242.1	−78.3	0.81	50	216.4	−72.9	0.92	R
34-2, 106-108	208.56	336.1	−0.09	NRM					R?
35-1, 120-122	210.20	77.4	29.4	0.22	100	56.8	32.0	0.12	N
35-1, 128-130	210.3	31.2	0.11	NRM					N

Note: D = declination, I = inclination, Int = intensity; NRM = natural remanent demagnetization; N = normal, R = reversed polarity.

further movement. This suggests that a secondary component of normal polarity has been removed by the low alternating fields.

Magnetic Polarity Record

A polarity reversal record could not be developed for the upper part of this hole, but it could be achieved for the older sediments, and the results are summarized in Figure 6. The position of the nannofossil and foraminiferal zones (Müller, this volume and Snyder, this volume) are also shown on this diagram, together with the anomaly numbers assigned to each reversal. Unfortunately, the section is incomplete; there are gaps in the record between the early and middle Eocene and between the Eocene and Maestrichtian. An interesting feature is the normal polarity interval corresponding to nannofossil Zone NP10, which is not obviously correlated with any specific magnetic anomaly on the standard polarity time scales of Lowrie and Alvarez (1981) or Hailwood et al. (1979).

NRM Intensity and Volume Susceptibility Measurements

Figure 7 illustrates the downhole variation in volume susceptibility and NRM intensity in the lower part of Hole 548A. The abrupt upward lithologic change that occurs at 469.9 m sub-bottom between nannofossil chalks and overlying brown-colored marly nannofossil chalks is correlated with a sudden increase in volume susceptibility and NRM intensity. Similarly, the distinct decrease in susceptibility and NRM intensity at 412.6 m sub-bottom corresponds to an abrupt lithologic change between the early Eocene marly nannofossil chalks and middle Eocene light-colored chalks. The increase in susceptibil-

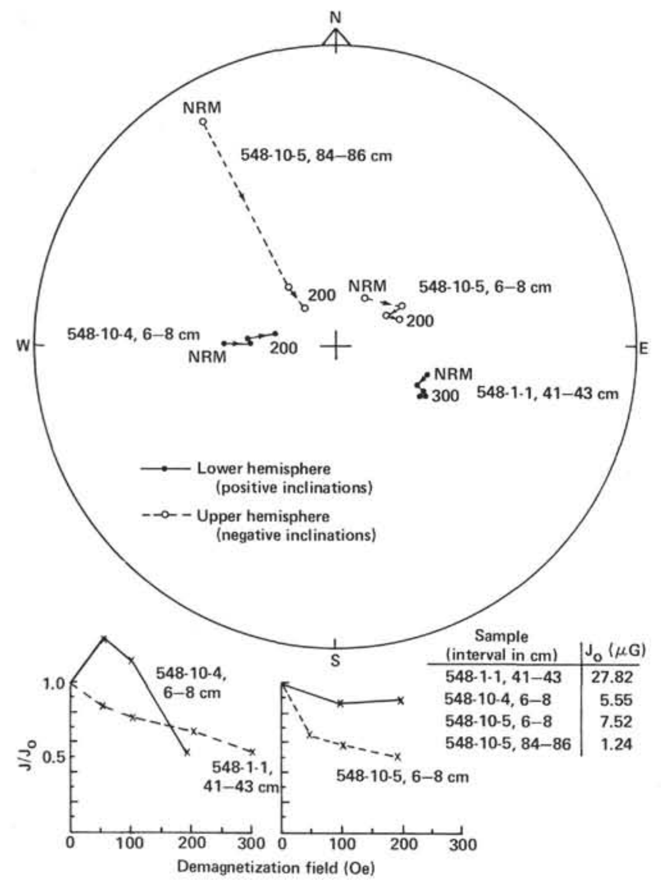

Sample (interval in cm)	J_0 (μG)
548-1-1, 41–43	27.82
548-10-4, 6–8	5.55
548-10-5, 6–8	7.52
548-10-5, 84–86	1.24

Figure 2. Behavior of four samples from Hole 548 during af demagnetization. Numbers refer to the peak applied alternating field in oersteds. The graphs illustrate the change in normalized intensity with peak demagnetization field for these samples; J = intensity, J_0 = initial intensity.

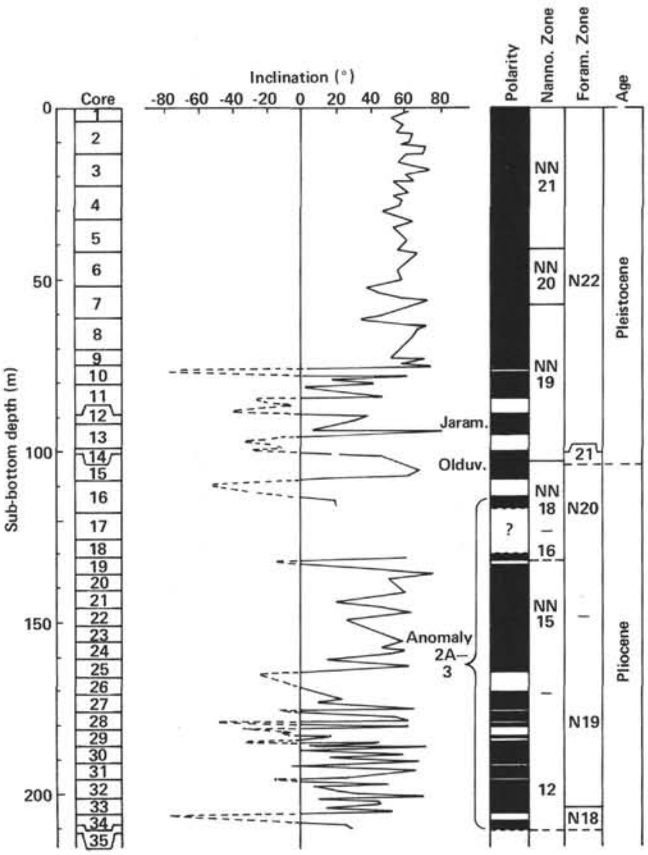

Figure 3. Downhole variation of magnetic inclination and inferred polarity reversal sequence for Hole 548. Positions of biostratigraphic zones are also shown. Normal polarity intervals shaded, reverse white.

ity and NRM intensity values at 469.9 m sub-bottom would seem to represent an increase in the supply of terrigenous material that ceased at the end of the early Eocene. The change is of particular interest because similar results were noted at Holes 400A and 401 during DSDP Leg 48 (Fig. 8). At Hole 400A this magnetic boundary occurs at a depth of 565 m, and at Hole 401 it occurs at 173 m. Magnetic fabric studies suggest that important changes in the direction of sediment transport might correspond to these fluctuations in lithology and magnetic intensity (Hailwood and Folami, this volume).

Site 549

At Site 549 (the second shallowest site in the Goban Spur transect), two holes were drilled near the seaward edge of the tilted block of Hercynian basement. For Hole 549A the VLHPC was used, and a sequence of Holocene to middle Eocene nannofossil and marly nannofossil oozes was recovered. Hole 549 was rotary drilled, and middle Eocene to lower Barremian chalks, mudstones, sandstones, and limestones were recovered; they rest on Hercynian basement.

Paleomagnetic Results

Approximately 400 samples were taken from Site 549; the results of the paleomagnetic measurements are listed in Table 3. At Hole 549A an abrupt change in NRM intensity occurs at the base of Core 3. This change corresponds to the hiatus between the Pleistocene marly sediments and the underlying sequence of nannofossil oozes. Since the nannofossil oozes were very weakly magnetized, the results for this section are largely based on NRM measurements or demagnetization in very low alternating fields.

Figure 9A illustrates the behavior upon demagnetization of typical samples from Site 549. Figure 9A shows a normal polarity sample (549A-3-4, 33–35 cm) and a reverse polarity sample (549A-3-1, 19–21 cm) from Hole 549A. The latter clearly demonstrates that a secondary component is removed on demagnetization. Figure 9B shows two normal polarity samples and two reverse polarity samples from Hole 549. The results are broadly similar to those from Hole 549A. A histogram of the magnetic inclinations of all the samples from Hole 549 after af demagnetization is shown in Figure 10. The histogram is bimodal, with the two peaks representing the normal and reverse polarity samples. The abundance of normal polarity samples is due to the long section through the Cretaceous magnetic quiet zone. The broken lines on the histogram indicate the theoretical axial geocentric dipole values for this latitude. For both the normal and reverse polarity samples, the peaks are displaced away from this value toward lower inclination

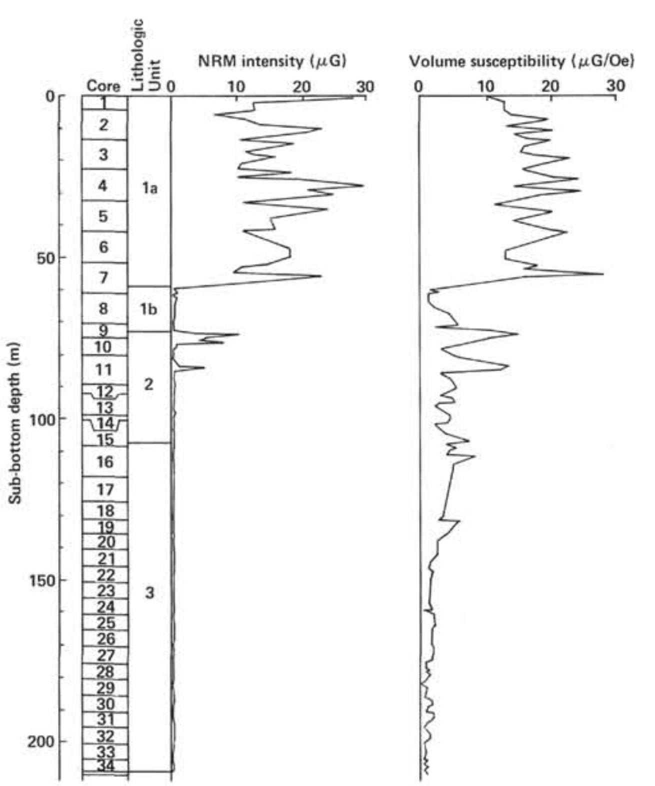

Figure 4. Correlation between volume susceptibility, NRM intensity, and lithology at Hole 548.

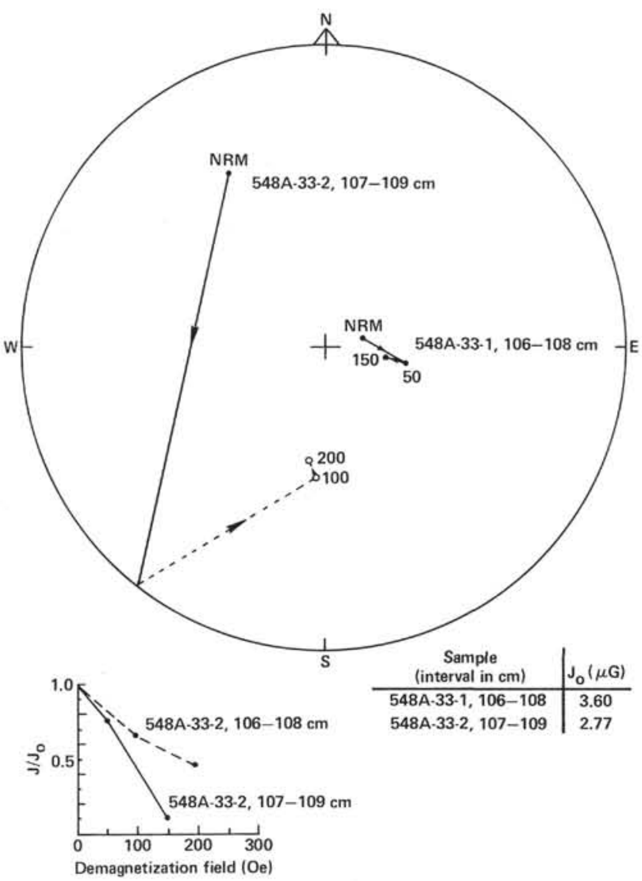

Figure 5. Demagnetization behavior of two representative samples from Hole 548A. Symbols as in Fig. 2.

values, probably as a result of the combined effects of compaction and the incomplete removal of secondary components of magnetization of normal polarity.

Hole 549A

The sequence of polarity reversals established at Hole 549A is shown in Figure 11. The Pleistocene sediments down to 24.00 m sub-bottom were of normal polarity, with the exception of one sample at 17.69 m sub-bottom. The results from the underlying sediments are less reliable because of the lower magnetic intensities of the nannofossil oozes. It has been impossible to establish a magnetostratigraphy for the Miocene sediments, because the section is highly condensed. The preceding section through the Oligocene and upper Eocene is more complete, and the magnetic polarity reversals deduced for this section are shown in Figure 11. It must be stressed that these results are based either on NRM measurements alone or (in the case of the slightly stronger samples) demagnetization in low alternating fields (up to 50 Oe). The biostratigraphy was used to assign magnetic anomaly numbers to the polarity reversals and to define gaps in the sequence. The results are significant, because they provide an opportunity to define the position of the Oligocene/Eocene boundary in this hole.

The position of the Oligocene/Eocene boundary in the magnetic polarity time scale is subject to some dispute. LaBrecque et al. (1977) place it in the reverse polarity interval preceding Anomaly 15, whereas Ness et al. (1980) propose that it lies at the top of Anomaly 16B. In the most recent study, Lowrie and Alvarez (1981) place it in the reverse polarity interval following Anomaly 15. The work of Lowrie and Alvarez (1981) is based on combined paleomagnetic and biostratigraphic studies of relatively complete sections of pelagic limestones in the Southern Appennines and is therefore likely to provide the best direct correlation between the magneto- and biostratigraphy. On this basis the Eocene/Oligocene boundary in Hole 549A may be placed between 120.00 and 123.4 m sub-bottom.

Hole 549

The paleomagnetic results from the upper part of Hole 549 (down to the Paleocene/Upper Cretaceous hiatus) span a sequence of richly fossiliferous sediments of middle Eocene to late Paleocene age. This section, which is ideally suited to detailed biostratigraphic studies, proved also to be suitable for magnetostratigraphic work. The downhole variation of magnetic inclination together with the polarity reversal sequence defined is shown in Figure 12. A series of polarity reversals has been defined that is believed to correlate with marine magnetic Anomalies 18 to 26.

It was thought at first that this section was complete, inasmuch as the biostratigraphic and magnetostratigraphic studies showed no direct evidence of breaks in

Table 2. Paleomagnetic results, Hole 548A.

Core-Section (interval in cm)	Sub-bottom depth (m)	Before demagnetization D (°)	Before demagnetization I (°)	Before demagnetization Int (μG)	Demagnetization field (Oe)	After demagnetization D (°)	After demagnetization I (°)	After demagnetization Int (μG)	Polarity
2-1, 117-119	216.17	133.0	29.9	0.035	NRM				N
2-2, 117-119	217.67	13.3	55.9	0.151	50	358.2	57.5	0.140	N
2-3, 27-29	218.27	9.2	−13.3	0.308	100	199.1	50.2	0.106	N
2-3, 122-134	219.32	281.7	80.5	0.398	NRM				N
2-4, 37-39	219.57	51.3	69.5	0.105	25	99.0	54.9	0.132	N
3-1, 68-70	225.18	4.0	37.1	0.059	NRM				N
3-1, 131-133	225.31	159.3	−1.9	0.458	75	156.5	−3.3	−.102	R?
3-2, 15-17	227.15	295.7	58.9	0.235	50	279.9	75.5	0.215	N
3-3, 109-111	228.59	15.6	64.9	0.223	50	183.2	58.5	0.165	N
3-4, 27-30	229.27	347.1	51.3	0.147	25	250.3	78.4	0 045	N
3-4, 118-121	230.18	202.8	33.6	0.083	NRM				N
3-5, 19-22	230.69	105.7	35.7	0.250	50	101.3	37.5	0.155	N
3-5, 111-113	231.61	158.8	−15.4	0.038	NRM				R?
3-6, 35-36	232.35	291.2	78.8	0.156	NRM				N
3-6, 104-107	233.4	117.7	72.0	0.200	25	48.0	57.0	0.196	N
4-2, 43-46	234.93	104.0	87.4	0.181	50	207.2	0.2	0.71	N
4-3, 42-45	236.42	180.9	71.8	0.107	NRM				N
4-4, 43-46	237.93	152.5	33.8	0.094	NRM				N
4-4, 108-111	238.58	22.7	61.0	0.009	NRM				N
4-5, 6-8	239.06	340.5	67.2	0.007	NRM				N
4-5, 120-122	240.20	320.0	−11.6	0.106	40	331.9	−32.9	0.119	R
4-6, 25-27	240.75	166.4	39.5	0.103	NRM				N
4-6, 124-126	241.74	8.3	4.3	0.043	NRM				N
5-1, 30-32	242.85	342.8	55.4	0.067	NRM				N
5-1, 116-118	243.66	348.2	47.8	0.009	NRM				N
5-2, 34-36	244.34	110.6	−31.5	0.005	NRM				R
5-2, 92-94	244.92	83.1	57.4	0.035	NRM				N
5-3, 92-94	246.37	127.8	48.9	0.005	NRM				N
5-4, 26-28	247.26	241.8	31.5	0.093	NRM				N
5-5, 88-90	249.38	42.1	73.7	0.015	NRM				N
5-6, 131-133	250.31	215.9	−45.1	0.006	NRM				R
6-2, 118-120	254.68	292.9	−45.1	0.006	NRM				R
6-3, 133-135	256.33	201.3	−39.3	0.020	NRM				R
6-4, 128-130	257.78	9.3	30.2	0.070	NRM				N
7-1, 137-139	262.87	70.7	−75.6	0.034	NRM				R
7-3, 55-57	265.05	150.3	−31.1	0.010	NRM				R
8-1, 96-98	272.96	304.7	56.7	0.049	NRM				N
8-2, 95-97	274.45	350.2	−18.6	0.009	NRM				R
8-3, 55-57	275.55	29.8	31.8	0.052	NRM				N
8-3, 90-92	275.90	149.9	−27.3	0.010	NRM				R
8-1, 67-69	280.17	338.9	17.5	0.265	NRM				N
9-2, 28-30	383.25		61.3	0.295	40	355.5	40.3	0.245	N
9-2, 106-108	284.06	51.0	31.2	0.061	NRM				N
9-3, 108-110	285.58	1.7	−27.4	0.117	25	56.3	15.2	0.09	?
9-4, 28-30	286.28	29.7	39.1	0.053	NRM				N
9-4, 120-122	287.20	302.1	−16.8	0.253	25	277.3	−3.7	0.22	R
9-5, 163-165	288.13	6.3	37.9	0.164	25	316.6	39.2	0.120	N
9-5, 120-122	288.7	46.6	34.3	0.011	NRM				N
10-2, 49-50	292.99	24.5	51.9	0.295	25	10.3	60.7	0.358	N
10-2, 94-96	293.44	333.3	25.4	0.030	NRM				N
10-3, 34-36	294.34	59.7	58.1	0.241	50	59.3	71.2	0.210	N
10-3, 118-120	295.18	333.1	45.0	0.049	NRM				N
10-4, 34-36	295.84	266.4	73.6	0.101	NRM				N
10-5, 36-38	297.36	325.3	68.5	0.178	50	170.1	39.6	0.019	N
10-6, 32-34	298.82	349.4	46.4	0.100	NRM				N
10-6, 123-125	299.73	62.7	19.4	0.060	NRM				N
11-1, 101-103	301.51	69.8	0.8	0.029	NRM				N
11-2, 40-42	302.40	322.2	72.8	0.062	NRM				N
11-2, 97-99	302.97	319.1	9.5	0.133	NRM				N
11-3, 27-29	303.79	300.6	43.6	0.054	NRM				N
11-3, 108-110	304.08	287.9	70.9	0.121	25	223.1	26.3	0.043	N
11-4, 48-50	305.48	51.3	−42.6	0.011	NRM				R
11-4, 135-137	306.35	356.1	−16.8	0.022	NRM				R
11-5, 19-21	306.69	102.3	83.2	0.065	NRM				N
12-1, 25-27	310.25	329.2	−10.9	0.036	NRM				R
12-2, 127-129	312.79	132.5	−19.0	0.081	NRM				R
12-3, 126-128	314.26	200.4	35.7	0.100	NRM				N
12-4, 116-118	315.66	9.5	53.0	0.064	NRM				N
12-5, 138-141	317.39	246.5	−21.1	0.047	NRM				R
12-6, 9-11	317.59	233.7	−46.1	0.130	NRM				R
13-1, 28-30	319.80	117.8	77.7	0.020	NRM				N
13-1, 136-138	320.86	75.0	−29.5	0.057	NRM				R
13-2, 25-28	321.25	194.7	−25.5	0.021	NRM				R
13-2, 133-136	322.33	14.6	−42.3	0.001	NRM				R
13-3, 16-19	322.66	46.3	72.6	0.002	NRM				N
13-3, 114-116	323.64	339.4	−23.7	0.075	NRM				R
13-4, 9-12	324.09	293.6	23.3	0.063	NRM				N
13-4, 116-119	325.16	2.2	−46.6	0.057	NRM				R
13-5, 23-25	325.73	195.5	39.8	0.040	NRM				N
13-5, 144-146	236.94	117.6	−4.5	0.041	NRM				R
13-6, 35-38	327.35	193.7	13.3	0.762	NRM				N
13-6, 133-136	328.33	154.1	84.3	0.005	NRM				N
14-1, 15-17	329.15	337.2	27.6	0.075	NRM				N
14-1, 123-125				0.001	NRM				N
14-2, 15-17	330.65	274.8	−15.5	0.002	NRM				R
14-2, 98-100	331.48	321.8	−43.6	0.042	NRM				R
14-3, 37-39	332.37	120.2	34.4	0.061	NRM				N
14-3, 122-124	333.22	228.2	37.6	0.002	NRM				N
14-4, 33-35	333.83	11.7	−47.0	0.058	NRM				R
14-4, 115-117	334.15	279.5	17.9	0.108	NRM				N

Table 2. (Continued).

Core-Section (interval in cm)	Sub-bottom depth (m)	Before demagnetization D (°)	Before demagnetization I (°)	Before demagnetization Int (μG)	Demagnetization field (Oe)	After demagnetization D (°)	After demagnetization I (°)	After demagnetization Int (μG)	Polarity
14-5, 31–33	335.31	359.2	26.1	0.043	NRM				N
14-6, 81–83	337.1	320.0	53.1	0.105	NRM				N
15-1, 133–135	339.83	56.0	−21.0	0.132	25	214.2	42.2	0.193	N
15-2, 45–47	340.45	301.6	2.0	0.104	NRM				N
15-2, 108–110	341.08	47.8	10.3	0.047	NRM				N
15-3, 116–118	342.66	26.5	−8.5	0.022	NRM				R
15-4, 48–50	343.48	352.5	−40.9	0.005	NRM				R
15-5, 25–27	344.75	80.3	41.2	0.166	50	129.4	14.7	0.135	N
15-6, 12–14	346.12	304.3	67.0	0.092	NRM				N
16-1, 28–31	349.21	254.3	11.2	0.099	NRM				N
16-2, 19–21	349.69	298.5	66.5	1.709	50	288.5	62.2	1.363	N
16-3, 26–29	351.26	41.8	62.9	6.4	150	57.2	60.9	1.604	N
16-4, 19–21	352.69	353.7	−6.4	1.207	100	309.3	−49.8	1.048	R
16-4, 119–121	353.69	215.4	72.2	3.689	50	189.3	74.6	1.947	N
16-5, 20–22	354.20	148.5	82.2	1.122	75	17.2	−57.0	0.87	R
17-1, 32–34	357.82	138.6	57.0	2.439	100	110.9	52.5	0.384	N
17-1, 116–118	358.66	219.4	79.4	3.806	75	280.0	80.2	0.992	N
17-2, 123–125	360.23	33.7	67.0	2.73	NRM				N
17-3, 34–36	360.84	102.7	63.4	8.255	100	110.7	62.5	2.523	N
17-4, 106–108	363.06	187.7	69.2	9.109	100	199.7	66.2	4.585	N
17-5, 114–116	365.14	61.6	57.7	7.164	100	62.2	52.1	1.967	N
17-6, 130–133	366.30	27.0	63.3	4.697	100	14.7	78.7	1.090	N
18-1, 25–27	367.25	242.9	62.3	9.608	100	242.1	62.9	4.558	N
18-2, 101–103	369.51	296.7	72.7	6.887	100	165.8	73.6	0.765	N
18-3, 32–34	370.32	91.3	81.8	2.405	50	52.9	77.4	1.119	N
19-1, 25–27	376.75	352.8	18.2	0.191	50	300.0	29.6	0.070	N
19-1, 144–146	377.94	12.9	14.1	0.094	50	357.8	56.7	0.085	N
19-2, 16–19	378.16	185.6	−33.2	0.096	NRM				R?
19-3, 130–132	380.80	194.1	57.3	0.216	50	112.5	47.7	0.126	N
19-4, 34–37	381.34	189.1	61.8	0.082	NRM				N
19-4, 108–111	382.08	100.1	83.3	0.361	50	87.7	74.3	0.187	N
19-5, 18–21	382.68	291.5	48.5	0.204	25	307.9	34.2	0.094	N
19-5, 105–107	383.55	46.1	58.6	0.635	100	94.7	55.6	[illegible]	N
19-6, 35–37	384.35	116.0	42.1	0.003	NRM				N
19-6, 95–97	384.95	9.1	−30.6	0.095	NRM				R
20-1, 108–110	387.08	282.3	13.8	0.086	NRM				N
20-2, 20–23	387.70	354.1	−30.2	0.001	NRM				R
20-2, 109–111	388.59	311.9	−4.4	0.056	NRM				R
20-3, 27–30	389.27	219.6	85.8	0.155	NRM				N
20-4, 11–13	390.61	106.4	47.3	0.316	25	313.3	−55.8	0.062	R
21-1, 23–25	395.73	83.8	−33.7	0.061	NRM				R
21-1, 109–111				0.103	NRM				R
21-2, 46–48	397.46	105.1	23.1	0.181	25	70.2	67.4	0.133	N
21-3, 19–21	398.69	10.3	20.8	0.124	25	21.9	43.6	0.143	N
21-3, 107–109	399.59	32.4	−8.1	0.121	NRM				R
21-4, 15–19	400.13	338.2	23.6	0.125	25	84.4	−29.7	0.050	R
21-4, 125–127	401.25	28.0	3.1	0.144	NRM				N
22-1, 13–16	405.13	114.8	67.7	0.408	25	147.5	66.3	0.230	N
22-2, 13–16	406.63	120.7	77.7	0.436	25	165.3	74.8	0.205	N
22-3, 25–28	408.25	301.7	57.0	1.729	50	302.7	48.4	1.415	N
22-4, 22–25	408.72	199.5	73.2	3.966	100	200.8	62.2	1.811	N
22-5, 32–35	411.32	194.1	66.5	6.267	200	180.0	45.5	3.548	N
22-5, 128–131	412.28	8.2	42.1	1.830	200	92.9	40.3	1.386	N
22-6, 92–95	413.42	40.7	61.5	12.108	200	22.1	−21.9	1.279	R
23-1, 24–26	414.74	6.6	41.5	33.928	500	357.4	8.4	4.907	R?
23-1, 111–113	415.63	306.8	15.7	28.579	300	291.3	−0.0	4.428	R
23-2, 49–51	416.49	66.7	40.3	44.137	500	56.3	9.1	9.405	R
23-2, 112–114	417.12	239.6	5.8	12.665	300	213.0	4.9	4.238	R?
23-3, 29–31	417.79	287.4	−11.9	29.543	300	275.5	−34.2	14.122	R
23-3, 126–128	418.76	320.4	−8.8	17.397	300	298.3	−29.5	6.638	R
23-4, 98–100	419.98	239.5	49.8	11.867	300	238.9	−7.0	5.842	R
24-1, 73–75	425.73	191.6	−5.6	30.121	400	192.1	−20.4	12.173	R
24-2, 84–86	427.34	7.8	−23.4	10.636	500	357.5	5.8	3.877	?
24-3, 36–38	428.36	168.7	42.2	11.362	300	202.4	−12.8	4.857	R
24-4, 38–40	429.38	202.4	−12.8	4.857	NRM				R
24-5, 93–95	431.93	111.4	−11.0	10.298	NRM				R
24-6, 66–68	433.16	170.0	16.8	17.228	400	185.8	−23.2	9.003	R
25-1, 22–24	433.72	243.2	38.9	11.391	400	234.2	−25.9	4.641	R
25-2, 120–122	436.22	186.1	−23.2	17.006	400	190.9	−43.4	8.77	R
25-3, 118–120	477.68	247.6	71.3	23.004	400	257.8	40.8	3.882	N
25-4, 37–39	438.37	277.0	33.4	15.797	300	274.9	30.1	4.385	N
25-4, 114–116	439.14	136.4	19.0	50.411	500	123.6	−0.1	13.85	R
25-5, 125–127	440.75	175.5	55.5	38.795	500	274.2	48.9	11.772	N
26-6, 16–18	450.66	327.4	42.3	57.201	400	332.0	34.2	12.646	N
27-1, 53–55	453.03	27.4	−20.5	8.871	200	28.4	−46.6	9.460	R
27-2, 29–31	454.29	75.9	61.4	7.225	200	93.8	50.3	1.772	N
27-2, 111–113	455.11	92.1	55.2	14.727	600	110.0	23.8	2.477	N
27-3, 42–44	455.92	184.5	54.6	17.335	300	188.1	45.5	6.559	N
27-4, 42–44	457.42	112.5	53.6	15.712	600	94.5	34.5	2.177	N
27-5, 38–40	458.88	285.7	72.2	34.249	400	292.6	54.6	7.284	N
27-5, 121–123	459.71	337.8	−24.3	3.125	200	213.8	−51.6	1.115	R
28-1, 28–30	463.28	29.0	40.1	2.485	150	0.7	−16.3	1.424	R
28-2, 31–33	463.8	32.3	72.1	13.973	200	293.7	66.6	2.876	N
28-2, 128–130	464.78	17.6	42.9	9.631	200	24.7	59.0	2.668	N
28-3, 40–42	465.40	228.5	68.7	19.249	700	317.9	24.0	3.041	N
28-3, 112–114	466.12	7.4	59.0	15.569	200	5.8	58.8	3.114	N
28-4, 38–40	466.88	93.8	65.5	11.77	300	254.2	−2.5	0.899	R
28-5, 35–37	468.35	119.2	67.2	26.017	300	289.9	−7.7	1.106	R
28-6, 19–21	469.69	228.6	79.1	10.611	100	230.6	−31.6	8.435	R

Table 2. (Continued).

Core-Section (interval in cm)	Sub-bottom depth (m)	Before demagnetization D (°)	Before demagnetization I (°)	Before demagnetization Int (μG)	Demagnetization field (Oe)	After demagnetization D (°)	After demagnetization I (°)	After demagnetization Int (μG)	Polarity
28-3, 18-20	471.18	19.3	24.6	3.519	50	23.4	−16.8	3.898	R
29-1, 33-35	471.83	64.3	50.1	1.449	150	82.3	−43.9	3.213	R
29-1, 88-90	472.38	8.1	71.1	1.627	200	319.6	11.7	0.249	R?
29-2, 46-48	473.46	92.6	81.1	6.185	100	115.9	79.4	4.085	N
29-2, 97-99	473.97	90.3	59.7	4.556	200	76.2	43.2	0.470	N
29-3, 24-26	474.74	26.5	−26.4	14.104	100	37.7	−26.9	14.294	R
29-3, 89-91	475.39	42.1	37.6	0.563	150	47.5	−63.3	0.387	R
29-4, 52-54	476.52	262.7	73.5	3.812	100	266.2	57.5	3.650	N
29-5, 53-55	478.03	127.4	56.9	3.831	100	133.0	56.9	2.181	N
30-1, 144-146	482.44	18.7	61.7	1.959	100	24.1	60.3	1.722	N
30-2, 125-127	483.75	146.5	73.9	3.579	100	141.0	69.4	4.040	N
30-3, 15-17	484.15	135.3	70.3	3.104	100	136.1	68.9	2.845	N
31-1, 27-29	490.77	69.5	54.8	3.381	100	71.5	53.3	2.710	N
31-2, 90-93	492.90	350.4	62.7	3.354	NRM				N
32-1, 52-54	500.52	15.0	59.7	3.267	200	319.7	−43.6	1.146	R
32-1, 113-116	501.13	66.5	67.9	1.455	100	306.5	−49.3	0.378	R
32-2, 31-34	501.81	343.7	53.0	6.095	100	132.5	69.0	0.235	N
32-3, 23-26	503.23	84.7	81.1	8.042	100	139.6	68.2	1.253	N
32-4, 43-45	504.93	354.8	59.9	5.023	75	134.9	68.5	0.161	N
33-1, 39-41	509.89	314.2	63.5	1.519	75	83.2	−14.9	0.502	R
33-1, 106-108	510.56	331.1	34.9	3.604	200	185.8	−58.7	1.655	R
33-2, 36-39	511.36	47.7	57.2	3.276	200	293.4	−56.4	2.207	R
33-2, 107-109	512.07	81.2	79.7	2.775	150	101.1	72.8	0.279	N
33-3, 120-123	513.70	26.4	33.4	5.314	150	79.9	−43.6	2.151	R
34-1, 42-45	519.42	318.3	53.7	13.204	200	281.6	56.0	0.498	N
34-1, 124-126	520.24	155.5	79.3	16.318	100	169.3	68.0	2.281	N
34-2, 135-138	521.85	1.8	67.4	12.543	100	354.1	67.7	2.145	N
34-3, 45-48	522.45	36.5	34.6	4.792	200	291.7	−50.2	3.002	R
34-3, 105-108	523.05	324.8	60.7	9.752	100	82.2	28.0	0.260	?
34-4, 115-118	524.65	146.7	77.2	10.008	100	162.9	60.4	1.510	N
34-5, 116-119	526.16	115.4	51.2	9.104	50	131.5	50.3	4.118	N
34-6, 112-114	527.62	290.8	66.9	8.674	50	279.8	67.0	4.202	N
34-7, 11-14	528.11	296.0	−71.7	8.139	50	261.6	−74.0	4.576	R
35-1, 27-29	528.77	343.0	61.4	14.277	50	335.1	62.1	8.728	N

Note: Symbols and abbreviations as in Table 1.

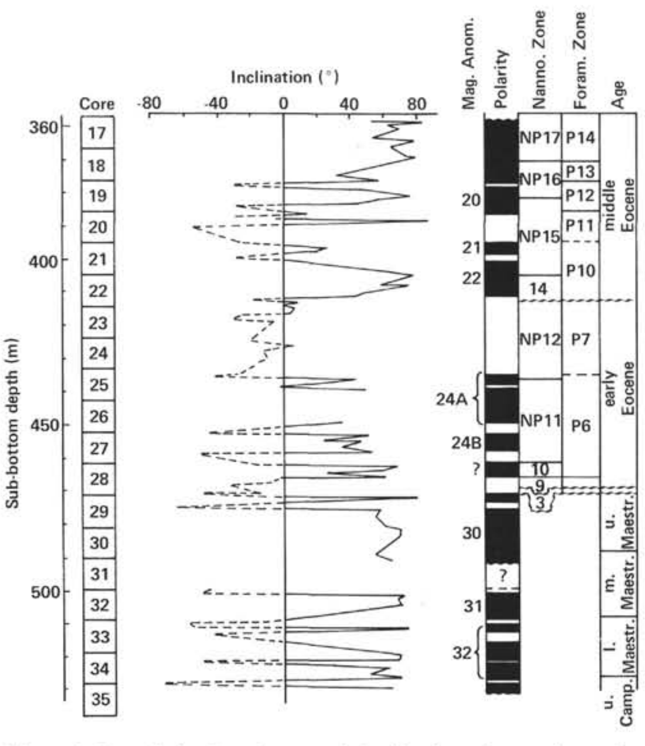

Figure 6. Downhole plot of magnetic inclination after optimum demagnetization and inferred polarity reversal sequence for Hole 548A.

sedimentation. However, at this site nannoplankton Zone NP10 is unusually short compared with the overlying zones. Furthermore, more than 45 thin bentonite layers have been recognized at this level at Site 550, but they do not appear to be present at Site 549 (Knox, this volume). This suggests that the upper part of nannoplankton Zone NP10 is probably absent at Site 549.

The sequence below the Paleocene/Maestrichtian hiatus is less complete. Figure 13 shows the paleomagnetic results for the cores that were sampled. The two normal polarity intervals in the Maestrichtian and Campanian are thought to represent Anomalies 32 and 33, respectively. They are preceded by a long normal polarity interval that extends from the top of the Santonian to the lower Barremian. In this long Cretaceous normal polarity interval three short polarity reversals (each one represented by only a single sample) were detected in Cores 37, 48, and 83, respectively. The upper two are of mid-Albian age, and the lower one is Barremian. Anomaly MO was not identified in this section but probably corresponds to the hiatus between early Albian and Barremian sediments. The paleomagnetic results from this hole indicate that the base of the Cretaceous quiet zone was not reached at Site 549. Thus, according to the van Hinte (1976) polarity time scale, which places the base of the Cretaceous normal polarity interval close to the base of the Barremian, the sediments lying directly above basement at Site 549 are not older than Barremian in age.

NRM Intensity and Volume Susceptibility

Figure 14 shows graphs of the downhole variation of NRM intensity and volume susceptibility. The general increase in NRM intensity and volume susceptibility below Core 8 corresponds to the lithologic change between light-colored nannofossil chalks and brown and gray nannofossil chalks. This increase in both properties in nannoplankton Zone NP14 agrees with the results from Site 548 and Hole 400A of Leg 48.

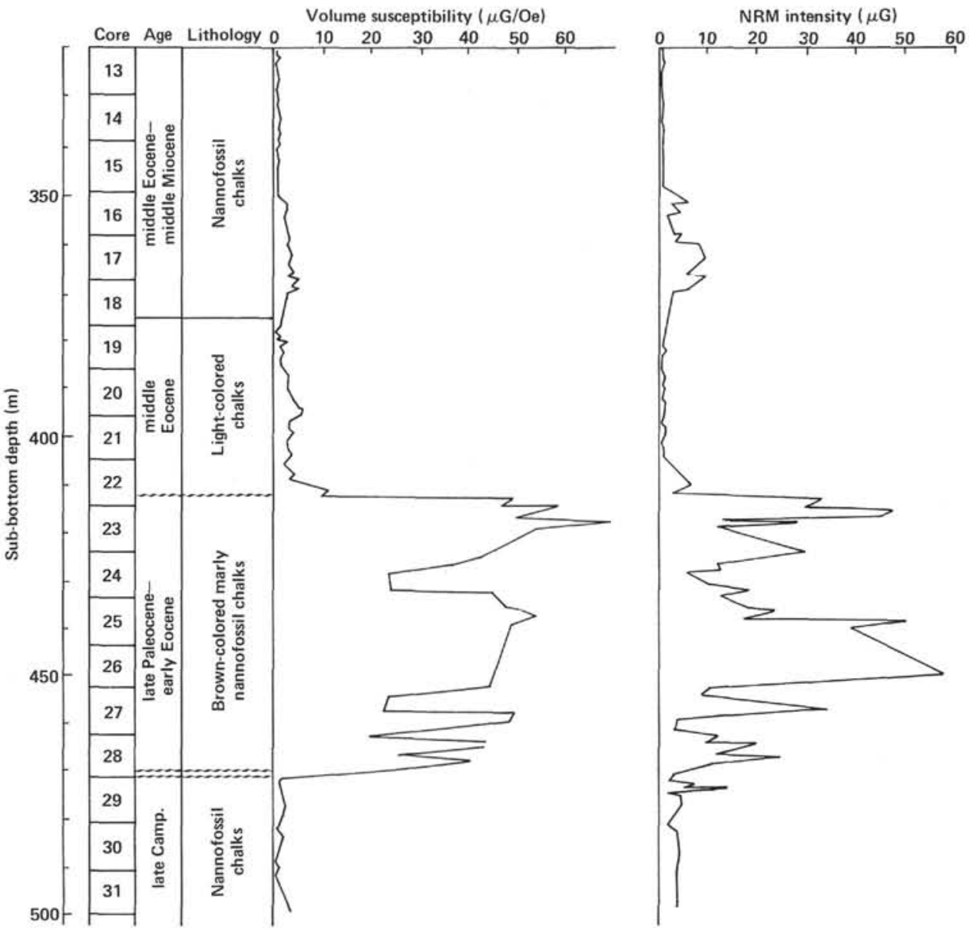

Figure 7. Correlation between volume susceptibility, NRM intensity, and lithology at Hole 548A. Interval between unconformities in Core 28 is early Paleocene in age.

Site 550

At Site 550 two holes (550 and 550B) were rotary drilled on the Porcupine Abyssal Plain. This site was at the greatest water depth of the sites drilled in the transect across the Goban Spur. Hole 550 was first washed to 99.5 m sub-bottom and then rotary drilled to a depth of 527 m. Hole 550B was washed to 456 m sub-bottom and then continuously cored to 720.5 m sub-bottom. The overlap between the two holes drilled at Site 550 resulted in the acquisition of a complete section across the Cretaceous/Tertiary boundary. The sediments recovered at this site were a sequence of Pliocene to late Albian nannofossil chalks and mudstones resting on oceanic basement. Hiatuses occur in the Miocene and early Oligocene to middle Eocene.

Paleomagnetic Measurements

Approximately 350 samples were measured from Site 550, and the paleomagnetic results for these samples are summarized in Table 4. The demagnetization behavior of representative normal and reverse polarity samples is shown in Figure 15. As with the samples from the previous two sites, the reverse polarity samples possess a low-coercivity component of normal polarity that is removed by demagnetization in low alternating fields. The normal polarity samples maintain a well-defined direction with a positive inclination during af demagnetization in fields up to 200 Oe.

Polarity Reversal Stratigraphy

Graphs of the variation of magnetic inclination with depth for Holes 550 and 550B are shown in Figures 16 and 17, respectively. At Hole 550 a series of short normal polarity zones was identified in Cores 5 to 10; the zones span nannoplankton Zones NN15 to NN12 and foraminifer Zones N20 to N19 and are believed to represent the sequence of short normal polarity intervals that characterize Anomalies 2A and 3.

The recovery of the underlying Miocene deposits was relatively poor, and because of the high frequency of geomagnetic field reversals during the Miocene an unambiguous interpretation of the sequence of polarity reversals observed is not possible.

Three hiatuses have been identified from biostratigraphic evidence in the upper half of Core 24. The hiatuses represent a span of approximately 25 m.y., an interval that extends through the early Eocene into the Oligocene. The sediments below Core 24 had notably higher NRM intensities and volume susceptibilities, and recovery improved considerably, enabling the sequence of polarity reversals to be identified. These reversals

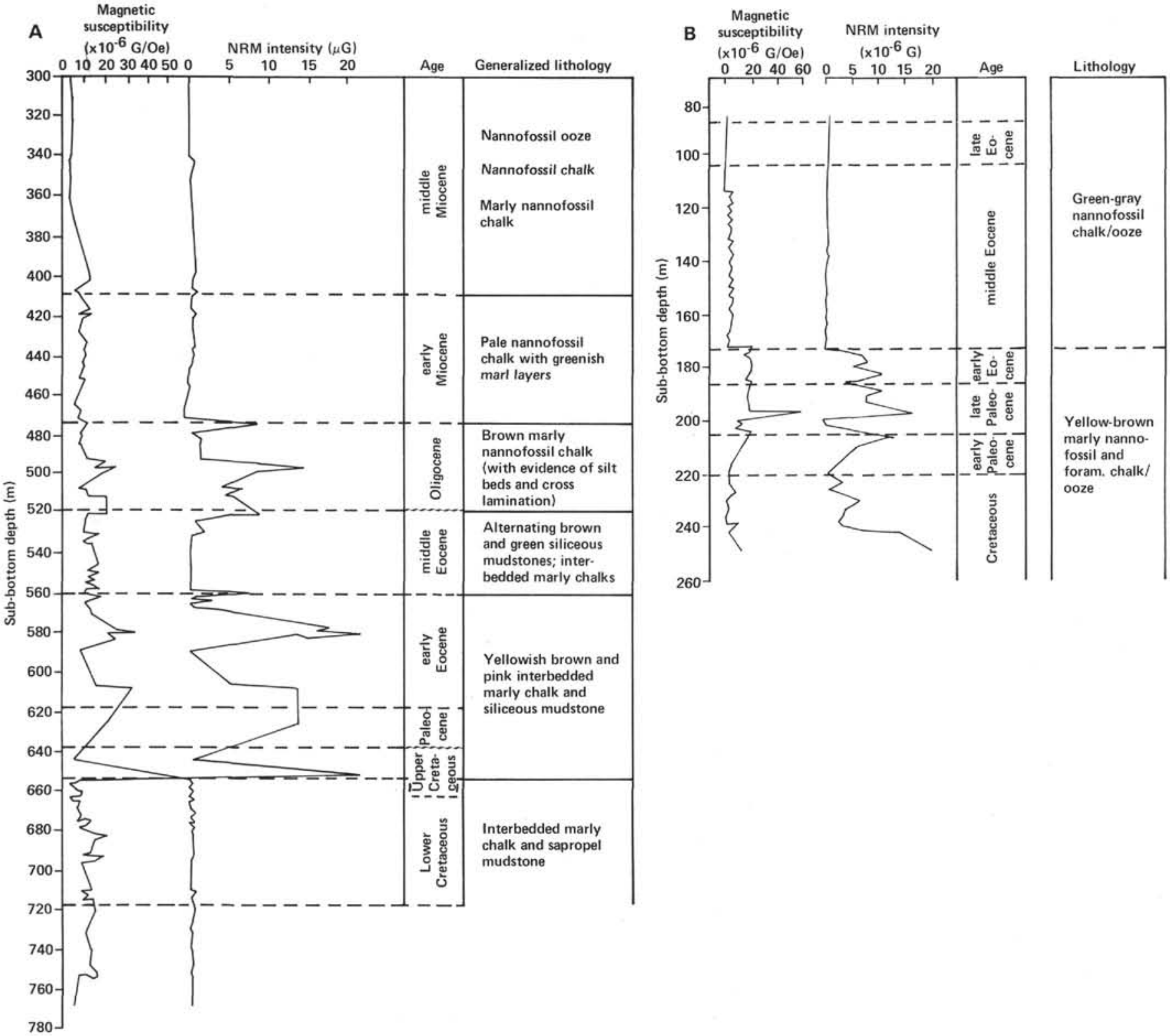

Figure 8. Leg 48 correlation between magnetic susceptibility, NRM intensity, and lithology. A. Hole 400A. B. Hole 401. (From Hailwood, 1979.)

span the Paleocene and early Eocene and are thought to represent Anomalies 22 to 27, although the section is incomplete because of a late Paleocene hiatus.

The identification of Anomalies 28, 29, and 30 was not straightforward in Hole 550, but fortunately the uppermost part of Hole 550B overlapped the lower part of Hole 550 so that the section from the Maestrichtian to early Paleocene was repeated. This permitted unambiguous identification of these anomalies in both holes. The position of Anomaly 29 is of particular interest, inasmuch as the Cretaceous/Tertiary boundary is generally accepted as lying within the reverse polarity interval immediately preceding this anomaly (Lowrie and Alvarez, 1981 and Hailwood et al., 1979). Detailed paleomagnetic sampling has allowed the base of Anomaly 29 to be defined within ± 2 cm at Hole 550B (between 469.67 and 469.71 m sub-bottom). This supports the micropaleontological interpretation that places the Cretaceous/Tertiary boundary in Hole 550B within Core 2, Section 3.

In Core 8 at Hole 550B a change in polarity was recorded in lithologic Subunit 3b (at 526.8 m sub-bottom) within sediments that were initially interpreted as a single thick turbidite unit. Further sampling confirmed the change in polarity and enabled its position to be precisely located (at 526.80 $\pm$ 0.02 m sub-bottom). The presence of a polarity reversal in this unit is inconsistent with the instantaneous emplacement of these massive light-colored beds. A more detailed examination of the core revealed the presence of fine banding in the vicinity of the polarity change that could represent a boundary between two separate turbiditic layers. This well-defined polarity change in Core 8 suggests the presence of a short reverse polarity interval within Anomaly 31.

Table 3. Paleomagnetic results, Site 549.

Core-Sample (interval in cm)	Sub-bottom depth (m)	Before demagnetization D (°)	Before demagnetization I (°)	Before demagnetization Int (μG)	Demagnetization field (Oe)	After demagnetization D (°)	After demagnetization I (°)	After demagnetization Int (μG)	Polarity
Hole 549A									
1-1, 18–20	0.18	99.5	71.4	5.568	50	114.8	73.1	4.848	N
1-2, 52–55	2.02	113.1	76.9	11.494	50	119.1	72.1	11.167	N
1-3, 47–50	3.47	95.8	71.0	10.622	50	103.1	63.4	10.567	N
1-4, 61–63	5.11	270.6	57.7	13.832	50	266.8	60.6	11.227	N
1-5, 26–29	6.29	98.7	71.0	12.785	50	103.8	69.5	10.239	N
2-1, 124–126	9.24	215.4	63.2	11.105	50	197.8	62.1	11.678	N
2-2, 124–126	10.74	309.7	37.3	16.102	50	299.7	41.0	15.493	N
2-3, 114–117	12.14	331.3	59.0	9.563	50	329.3	59.5	8.869	N
2-4, 35–38	12.85	229.8	46.0	9.497	50	227.1	43.9	8.615	N
2-5, 36–38	14.36	241.6	61.8	19.812	50	247.0	65.6	17.732	N
2-6, 38–40	15.88	238.0	52.5	26.364	50	235.7	54.7	24.902	N
3-1, 19–21	17.69	231.3	5.1	75.908	150	314.6	−21.1	30.463	R?
3-1, 115–117	19.64	321.9	72.6	10.211	200	350.4	80.6	6.934	N
3-2, 28–30	19.28	333.4	65.8	14.047	100	341.7	59.9	9.156	N
3-3, 52–54	21.02	158.7	77.3	5.674	50	181.9	69.4	3.907	N
3-4, 33–35	22.33	136.0	68.6	4.970	50	136.9	66.5	4.853	N
3-5, 50–52	24.00	67.2	70.5	21.084	50	68.0	69.5	18.684	N
3-5, 129–131	24.79	64.5	−25.7	1.429	150	297.4	−67.3	1.078	R
3-6, 69–71	25.69	253.4	−59.6	2.583	50	264.2	−73.4	3.496	R
4-1, 38–40	27.38	325.9	−48.2	0.155	25	237.4	−27.2	0.137	R
4-2, 38–40	28.88	101.9	−16.0	0.009	NRM				R
4-2, 106–108	29.56	276.6	29.9	10.039	NRM				N?
4-2, 38–40	30.38	112.3	2.6	0.027	NRM				R?
4-3, 136–138	31.36	271.5	64.0	0.035	NRM				N
4-4, 38–40	31.88	39.5	−16.6	0.012	NRM				R
4-4, 119–121	32.69	264.4	51.3	0.050	NRM				N
4-5, 36–38	33.36	144.8	29.7	0.039	NRM				N
4-5, 117–119	34.17	359.0	38.5	0.022	NRM				N
4-6, 29–31	34.79	258.1	−9.8	24.208	50	234.6	−9.6	24.613	R
4-6, 116–118	35.56	208.7	−72.2	0.193	50	216.9	−55.6	0.141	R
5-1, 60–62	37.10	09.7	33.0	0.045	NRM				N
5-2, 62–64	38.62	95.6	13.4	0.031	NRM				N
5-3, 45–47	39.95	202.3	49.4	3.035	50	263.4	54.5	0.066	N
5-4, 40–42	41.40	152.6	44.1	0.056	NRM				N
5-4, 107–109	42.07	202.3	44.1	0.064	NRM				N
5-5, 46–48	42.96	71.7	−19.0	0.017	NRM				R?
5-5, 91–93	43.41	295.5	33.0	0.084	NRM				N
5-6, 45–47	47.45	339.3	69.9	0.065	NRM				N
5-6, 84–86	44.84	306.8	54.2	0.082	NRM				N
6-1, 120–122	47.20	268.7	62.1	0.176	25	130.7	−56.4	0.113	R
6-2, 40–42	47.90	249.1	−36.7	0.041	NRM				R
6-2, 122–124	48.72	312.4	42.3	0.022	NRM				N?
6-3, 68–70	49.68	283.5	14.4	0.034	NRM				?
6-3, 132–134	50.32	308.0	−31.6	0.043	NRM				R?
6-4, 54–56	51.04	66.4	−70.1	0.064	NRM				R
6-4, 105–107	51.55	83.4	−59.8	0.595	50	183.3	13.7	0.030	R?
6-5, 59–61	52.59	172.1	26.9	0.034	NRM				?
6-5, 120–122	53.20	325.0	−20.2	0.025	NRM				R
6-6, 48–50	53.48	113.9	−51.5	0.036	NRM				R
6-6, 99–101	54.49	146.2	−43.2	0.033	NRM				R
7-1, 47–49	55.97	349.9	−0.3	1.197	200	348.3	10.3	0.970	N
7-1, 103–105	56.53	309.1	54.5	0.550	75	297.0	40.2	0.453	N
7-2, 48–50	57.48	313.0	42.3	2.180	50	319.1	46.0	1.203	N
7-3, 101–103	59.51	324.1	55.0	2.762	50	327.8	55.7	3.007	N
7-4, 55–57	60.55	342.1	24.2	1.072	50	331.4	32.5	2.197	N
7-5, 58–60	62.08	346.4	45.3	3.189	50	349.3	52.7	4.723	N
7-5, 101–103	62.51	30.5	31.9	1.747	150	48.6	37.2	0.934	N
7-6, 55–57	63.55	69.1	42.3	0.260	50	71.0	52.1	0.190	N
7-6, 98–100	63.98	259.2	80.0	0.260	50	209.0	−25.9	0.029	R
8-1, 33–35	65.33	90.6	−4.6	0.088	NRM				R
8-2, 33–35	66.83	358.0	1.1	0.001	NRM				R
8-2, 122–124	67.72	248.0	−71.0	0.069	NRM				R
8-3, 33–35	68.33	278.7	47.8	0.002	NRM				N
8-4, 33–35	69.83	312.7	10.7	0.013	NRM				N
8-5, 33–35	71.33	108.6	24.6	0.038	NRM				N
8-6, 33–35	72.83	346.7	56.7	0.035	NRM				N
9-1, 23–25	74.73	174.3	−42.1	0.412	50	167.4	−31.2	0.038	R
9-1, 120–122	75.70	247.4	45.0	0.241	50	279.2	49.4	0.109	N
9-2, 23–25	76.23	314.2	25.9	0.003	NRM				N
9-2, 120–122	77.20	210.9	55.6	0.124	NRM				N
9-3, 23–25	77.73	117.6	−5.4	0.000	NRM				R
9-3, 120–122	78.70	206.9	27.7	0.095	NRM				N
9-4, 23–25	79.23	244.7	33.2	0.043	NRM				N
9-4, 120–122	80.20	112.8	51.1	37.06	150	116.0	27.0	1.052	N
9-5, 23–25	80.73	186.9	2.4	0.090	NRM				?
9-5, 120–122	81.70	7.7	−67.3	0.100	NRM				R
9-6, 23–25	82.23	74.5	−30.4	0.015	NRM				R
10-1, 46–48	84.46	144.9	−49.9	0.021	NRM				R
10-1, 125–127	85.25	291.9	−5.8	0.027	NRM				R?
10-2, 46–48	85.96	165.2	24.0	0.035	NRM				N
10-2, 125–127	86.75	215.4	−10.0	0.036	NRM				R
10-3, 46–48	87.46	30.3	−25.1	0.024	NRM				R
10-3, 125–127	88.25	306.5	8.5	0.027	NRM				N?
10-4, 46–48	88.96	188.3	72.2	0.068	NRM				N
10-4, 125–127	89.75	100.3	42.7	0.063	NRM				N
10-5, 46–48	90.46	358.1	54.2	0.036	NRM				R
10-5, 115–117	91.15	241.6	−39.7	0.117	NRM				R
10-6, 48–50	91.98	337.8	−43.7	1.758	50	355.9	−30.7	0.027	R

Table 3. (Continued).

Core-Sample (interval in cm)	Sub-bottom depth (m)	Before demagnetization D (°)	Before demagnetization I (°)	Before demagnetization Int (μG)	Demagnetization field (Oe)	After demagnetization D (°)	After demagnetization I (°)	After demagnetization Int (μG)	Polarity
Hole 549A (Cont.)									
10-6, 125-127	92.75	43.8	−52.8	0.206	50	344.5	−58.2	0.165	R
11-1, 58-61	94.08	253.7	21.9	0.045	NRM				N
11-2, 22-24	95.22	66.8	19.8	0.016	NRM				N
11-2, 112-115	96.12	260.5	−23.7	0.017	NRM				R
11-3, 49-52	97.0	230.2	−48.5	0.009	NRM				R
11-4, 52-54	98.52	262.4	−31.4	0.006	NRM				R
11-5, 51-54	100.01	184.9	−23.3	0.022	NRM				R
11-5, 118-120	100.68	193.9	−38.6	0.076	NRM				R
11-6, 54-57	101.54	41.6	14.8	0.021	NRM				N
11-6, 122-125	102.22	279.3	1.2	0.021	NRM				?
12-1, 36-39	103.36	270.4	8.8	0.176	25	268.2	−11.4	0.175	R
12-1, 115-118	104.15	191.3	−72.0	0.016	NRM				R
12-2, 48-51	104.98	178.2	1.2	0.071	NRM				N
13-1, 41-44	106.41	[illegible]	25.7	0.044	NRM				N
13-2, 43-46	107.93	[illegible]	−56.8	0.091	NRM				R
13-3, 41-44	109.41	125.1	−75.9	0.012	NRM				R
14-1, 44-47	111.44	82.7	−2.2	0.277	25	76.3	31.2	0.099	N?
14-1, 109-111	112.09	84.5	38.6	0.011	NRM				N
14-2, 35-38	112.85	170.1	36.3	0.405	25	133.6	48.2	[illegible]	N
15-1, 35-38	116.35	11.0	1.7	0.331	25	226.9	48.3	[illegible]	N
15-2, 24-27	117.74	98.1	−55.8	0.061	NRM				R
15,CC (24-27)	119.24	340.0	80.3	0.120	NRM				N
16-1, 56-59	120.06	30.7	−41.1	0.197	25	66.4	−39.7	0.302	R
16-1, 110-113	120.60	335.7	−9.6	0.099	NRM				R
17-1, 44-47	122.94	14.8	−24.0	1.242	25	13.8	−24.6	1.463	R
17-1, 91-93	123.41	37.8	53.2	0.044	NRM				N
17-2, 26-29	124.26	157.0	11.4	0.099	NRM				N
18-1, 84-87	126.34	154.1	66.3	0.440	25	248.2	63.5	0.451	N
21-1, 47-49	129.47	111.9	−81.3	0.329	25	53.9	62.0	0.023	?
24-1, 46-48	132.46	206.3	−36.0	0.080	NRM				R
24-1, 86-88	132.86	96.4	−29.8	0.089	NRM				R
24-2, 28-30	133.78	237.5	72.8	0.152	NRM				N
25-1, 35-38	135.35	165.4	−36.6	0.248	25	83.4	−23.8	0.252	R
25-2, 26-28	136.76	119.4	26.6	0.298	50	22.1	41.0	0.826	N
25-2, 97-99	137.47	166.9	−32.9	0.058	NRM				R
26-1, 54-55	138.03	224.6	37.6	0.029	NRM				N
27-1, 52-54	139.02	268.3	61.4	0.184	25	204.9	20.2	0.133	N
27-1, 112-114	139.62	197.8	59.5	0.067	NRM				N
28-1, 27-30	140.27	66.0	−8.6	0.118	NRM				R
28-2, 30-32	141.80	162.9	14.7	0.165	25	246.0	74.8	0.263	N
32-1, 44-46	147.94	168.5	28.0	0.208	25	174.3	−8.3	0.128	R
32-1, 114-116	148.64	136.4	−20.2	0.149	NRM				R
32-2, 19-21	149.19	140.3	−2.8	0.246	25	170.1	−23.3	0.310	R
32-2, 84-86	149.84	185.4	−55.8	0.038	NRM				R
33-1, 42-44	150.92	91.1	75.8	0.153	25	58.6	57.8	0.170	N
33-1, 114-116	151.64	43.2	44.9	0.067	NRM				N
33-2, 42-44	152.42	80.4	42.9	0.173	25	69.8	−24.4	1.266	R
33-2, 114-116	153.14	185.4	−55.8	0.038	NRM				R
34-1, 38-40	155.88	217.1	−33.9	0.121	NRM				R
34-1, 120-123	156.20	316.8	−44.5	0.126	NRM				R
35-1, 38-40	160.88	166.8	78.8	0.089	NRM				N
36,CC (12-14)	170.12	31.6	071.7	0.037	NRM				R
37,CC (20-22)	175.20	345.1	−40.1	39.546	50	343.8	−41.0	42.10	R
38-1, 23-25	175.73	100.4	−17.9	0.029	NRM				R
39-1, 38-40	180.88	87.4	−24.6	0.069	NRM				R
39-1, 120-123	181.70	356.1	42.1	0.102	NRM				N
39-2, 38-40	182.38	0.7	−38.9	0.062	NRM				R
40-1, 25-27	185.75	338.1	−19.7	0.014	NRM				R
40-1, 104-106	186.54	280.0	21.6	0.091	NRM				N
Hole 549									
2-1, 113-116	199.63	174.0	5.5	0.023	NRM				R?
2-1, 121-123	199.71	358.1	2.4	0.060	NRM				R?
2-1, 132-134	199.82	344.5	67.1	0.019	NRM				N
2-2, 31-35	200.31	286.4	−35.3	0.019	NRM				R
2-2, 125-127	201.25	201.8	59.1	0.040	NRM				N
2-3, 113-116	202.63	23.4	59.0	0.244	50	86.7	42.0	0.099	N
2-4, 32-35	203.32	308.6	40.4	0.252	75	327.2	38.2	0.120	N
2-5, 107-109	206.57	140.0	−65.8	0.035	NRM				R
3-1, 23-25	208.23	228.5	68.3	0.214	75	317.6	52.2	0.082	N
3-1, 136-138	209.36	77.0	−9.4	0.019	NRM				R
4-1, 34-37	217.84	213.4	29.8	0.040	NRM				N
4-1, 139-141	218.89	302.5	−24.4	3.556	50	214.8	−18.1	5.831	R
4-2, 133-136	220.33	49.4	−20.6	34.188	50	44.2	−35.0	34.806	R
4-3, 55-58	221.05	310.4	−40.0	0.384	NRM				R
4-4, 24-26	222.26	352.8	−21.5	0.077					R
4-5, 19-21	224.69	100.3	48.3	0.038	NRM				N
4-6, 31-33	225.31	308.5	49.8	0.041	NRM				N
4-7, 39-41	226.89	161.5	30.7	0.064	NRM				N
5-1, 27-30	227.27	114.9	68.4	0.149	25	2.5	40.6	0.073	N
5-2, 132-134	229.82	32.0	51.3	0.103	25	216.0	70.6	0.033	N
5-3, 131-133	231.31	315.6	36.0	0.124	NRM				N
5-4, 111-113	232.61	69.4	52.8	0.131	25	74.0	52.0	0.195	N
5-5, 127-129	234.27	73.5	54.3	0.063	NRM				N
5-6, 127-130	235,77	156.4	29.2	0.149	25	166.7	57.9	0.175	N
5-7, 43-46	236.43	66.4	16.7	0.282	25	45.6	45.4	0.246	N
6-1, 90-92	237.40	7.2	73.6	0.309	50	20.9	40.6	0.187	N
6-2, 90-92	238.90	296.0	29.3	0.182	25	336.6	25.9	0.084	N
6-3, 38-40	239.88	28.4	56.5	0.136	25	48.7	49.7	0.182	N

Table 3. (Continued).

Core-Sample (interval in cm)	Sub-bottom depth (m)	Before demagnetization D (°)	I (°)	Int (μG)	Demagnetization field (Oe)	After demagnetization D (°)	I (°)	Int (μG)	Polarity
Hole 549 (Cont.)									
6-4, 50–52	241.50	192.5	12.9	0.051	NRM				R?
6-5, 21–23	242.71	31.4	5.4	0.041	NRM				R?
6-5, 83–85	243.33	10.6	19.7	0.151	25	356.6	32.3	0.096	R?
6-6, 83–85	244.83	347.0	−0.7	0.030	NRM				R
7-1, 13–15	246.13	5.0	50.7	0.094	NRM				N
7-1, 123–125	247.23	168.3	−37.7	0.132	25	225.0	−32.1	0.155	R
7-2, 8–10	247.58	343.1	−12.7	0.092	NRM				R
7-2, 100–102	248.5	51.4	−39.3	0.152	NRM				R
7-3, 109–111	250.9	8.6	40.8	0.975	NRM				N
7-5, 8–10	252.08	58.9	−6.6	0.099	NRM				R
7-5, 129–131	253.29	143.5	12.1	0.056	NRM				N?
8-1, 127–129	256.77	169.4	46.3	0.004	NRM				N
8-2, 90–92	257.90	295.4	−43.7	0.442	25	229.1	0.4	0.095	R?
8-3, 47–49	258.97	341.3	3.6	0.104	NRM				?
8-3, 99–101	258.49	12.0	59.3	0.211	25	19.7	49.4	0.237	N
8-4, 24–26	260.24	27.2	−0.3	0.153	25	21.1	−9.8	0.162	R
8-4, 138–140	261.38	356.2	30.5	0.045	NRM				R
9-1, 17–19	265.17	43.8	−41.3	4.146	150	52.2	23.0	3.232	R
10-1, 105–108	275.55	305.9	60.0	10.189	50	253.1	64.3	6.014	N
10-2, 30–33	276.30	321.2	76.9	12.296	50	49.2	67.0	8.944	N
10-2, 92–95	276.92	133.5	−27.5	10.745	200	138.0	−34.1	11.381	R
10-3, 104–107	278.54	318.2	−7.9	6.021	50	313.8	−11.0	5.570	R
10-4, 117–120	280.17	6.6	−13.6	3.688	50	10.5	−31.8	3.940	R
10-5, 99–101	281.49	286.9	−37.6	9.769	50	278.0	−42.0	9.500	R
10-6, 97–100	282.97	70.5	−52.2	11.602	50	70.8	−54.7	11.326	R
10-7, 10–12	283.60	226.8	−11.2	6.873	50	224.3	−44.0	7.208	R
11-1, 27–30	284.27	78.2	−57.7	7.527	50	77.4	−56.9	7.799	R
11-4, 26–29	288.76	6.1	14.2	11.530	50	7.6	10.9	10.620	N
11-5, 123–126	291.23	11.8	18.8	3.413	50	14.3	2.6	2.978	N
11-6, 93–95	292.43	95.3	19.2	2.249	50	102.7	12.3	6.595	N
11-7, 19–22	293.19	85.3	45.8	18.536	50	88.4	37.4	17.451	N
12-1, 109–111	294.59	312.2	25.8	18.428	50	310.6	25.4	17.381	N
12-2, 94–97	295.94	211.0	21.0	5.263	500	185.7	−6.1	0.765	R
12-3, 9–12	296.59	219.1	36.4	14.783	100	217.1	34.1	13.446	N
12-4, 95–98				22.800	500	155.3	75.2	3.234	N
13-1, 26–29			28.1	5.937	100	156.1	−7.9	7.415	R
13-2, 132–135	305.82	294.6	13.9	5.430	100	292.2	−4.4	5.360	R
13-3, 27–29	306.27	24.4	68.2	7.470	100	319.9	47.7	1.241	N
13-4, 80–83	308.30	100.6	44.7	1.975	100	96.8	42.5	1.800	N
13-5, 44–46	309.44	135.0	36.8	1.817	50	135.7	31.6	1.615	N
13-6, 102–105	311.52	304.8	44.1	25.876	100	314.2	33.8	14.228	N
13-7, 12–15	312.12	268.3	32.9	28.832	400	288.2	23.8	3.171	N
14-1, 73–76	313.23	76.7	25.5	2.104	50	76.7	46.6	2.325	N
14-2, 128–131	315.28	270.9	38.2	3.703	350	278.7	19.9	0.522	N
14-3, 123–125	316.73	48.0	48.9	1.178	50	48.6	48.1	1.284	N
14-4, 16–19	317.16	121.9	49.3	0.154	50	112.5	47.6	0.118	N
14-4, 123–125	318.22	31.6	17.0	0.378	25	24.9	−4.0	0.378	R
14-5, 75–78	319.28	60.6	−51.9	0.039	NRM				R
14-6, 139–141	321.39	60.2	−44.9	4.695	50	62.7	−62.8	11.280	R
14-7, 2–5	321.52	251.7	74.0	7.751	100	250.8	−6.6	6.570	R
15-1, 9–11	322.09	26.6	−7.6	0.558	50	27.3	−14.9	0.763	R
15-1, 126–128	323.26	299.3	29.8	0.675	400	293.4	12.9	0.281	?
15-2, 25–27	323.75	10.5	18.8	0.674	100	4.4	−6.6	9.478	R
15-2, 109–110	324.58	229.3	−4.5	2.662	100	218.6	−16.7	2.047	R
15-4, 124–126	327.74	191.2	4.0	1.267	100	206.3	−21.1	1.281	R
15-5, 112–114	329.12	275.0	62.0	0.781	100	242.0	−15.1	0.304	R
15-6, 136–138	330.86	58.6	−26.5	0.447	100	119.0	−1.2	0.211	R
16-1, 15–17	331.65	7.6	−45.5	0.921	100	4.0	−77.0	0.883	R
16-1, 140–142	332.90	113.0	33.9	2.241	300	130.2	10.0	0.893	?
16-2, 141–143	334.41	157.0	63.8	1.714	100	134.9	−3.3	1.356	R
16-4, 28–30	336.28	356.1	73.8	28.795	500	253.1	−1.7	5.201	R
16-5, 44–46	337.94	165.0	56.7	8.878	150	179.1	−0.4		R
16-6, 127–129	340.27	253.5	46.3	8.474	150	228.8	−21.1	9.697	
16-7, 25–27	340.75	182.7	74.5	8.638	150	212.7	−20.6	9.624	R
17-1, 126–128	342.26	284.3	11.2	1.592	300	288.3	−12.4	1.419	R
17-2, 130–132	343.80	193.4	−11.6	1.234	100	179.5	−15.5	1.726	R
17-3, 118–121	345.18	113.1	−52.9	1.584	100	34.2	−21.7	1.867	R
17-4, 101–103	346.51	307.0	−14.0	3.610	100	312.2	−27.6	2.141	R
17-5, 113–115	348.13	145.0	−10.3	1.475	100	154.6	−11.4	1.229	R
17-6, 136–138	349.86	144.7	−11.2	14.094	100	143.9	−13.8	14.394	R
18-1, 103–105	351.53	149.2	14.6	3.675	200	145.0	6.5	1.982	N?
18-2, 21–23	352.21	20.2	16.3	1.088	150	19.1	14.6	1.297	N
18-2, 101–103	353.01	208.3	23.2	10.492	200	210.5	6.4	4.503	N
18-3, 31–33	353.81	30.0	26.1	7.847	200	39.7	18.0	3.797	N
18-3, 91–93	354.41	44.2	9.9	2.11	200	49.1	−0.6	0.645	R
19-1, 46–48	360.48	223.1	−20.3	0.581	50	217.7	−15.1	0.332	R
19-2, 55–58	362.05	247.2	−59.0	1.718	50	257.0	−24.0	1.438	R
19-3, 116–118	364.16	6.6	−6.8	0.610	50	352.9	−8.9	0.406	R
19-4, 12–14	364.62	244.0	22.8	0.210	50	231.4	43.4	0.210	N?
19-4, 115–117	365.65	205.3	−61.0	0.109	NRM				R
19-5, 26–28	366.26	22.4	−25.4	0.088	NRM				R
20-1, 10–12	369.60	27.6	−12.2	2.262	50	31.0	−21.6	3.242	R
20-2, 43–45	371.43	117.0	45.9	0.273	50	84.0	−21.4	0.117	R
20-3, 38–40	372.88	106.6	36.5	0.112	25	83.9	−14.2	0.219	R
20-3, 142–144	373.92	349.2	−10.1	0.160	50	355.5	−17.6	0.072	R
20-4, 31–33	374.31	88.8	27.0	0.454	25	50.2	41.9	0.599	N
20-5, 9–11	375.69	213.6	42.1	0.448	25	229.3	45.1	0.484	N
20-6, 15–17	777.15	220.0	65.6	0.092	NRM				N
21-1, 114–116	380.14	37.2	63.7	1.766	50	282.9	80.9	0.893	N

Table 3. (Continued).

Core-Sample (interval in cm)	Sub-bottom depth (m)	Before demagnetization D (°)	Before demagnetization I (°)	Before demagnetization Int (μG)	Demagnetization field (Oe)	After demagnetization D (°)	After demagnetization I (°)	After demagnetization Int (μG)	Polarity
Hole 549 (Cont.)									
21-2, 24–26	380.74	48.3	−16.0	0.215	25	207.5	−6.5	0.242	R
21-2, 83–85	381.33	211.4	−6.5	0.992	50	203.0	−5.8	1.133	R
21-3, 118–120	393.18	348.8	42.7	6.565	50	330.8	10.6	6.334	R?
22-1, 52–54	389.02	309.6	64.4	5.995	150	212.5	−26.3	0.900	R
22-1, 104–106	389.54	229.5	−16.5	6.212	200	204.8	−32.3	0.627	R
22-2, 32–34	390.32	212.8	62.7	13.192	300	219.5	40.6	2.346	N
22-3, 31–33	391.81	343.4	53.3	3.561	200	343.5	59.6	2.352	N
22-3, 131–133	392.81	157.2	73.3	3.137	200	35.5	16.2	0.228	N
22-4, 46–48	393.46	147.5	57.2	4.160	150	153.6	38.9	0.989	N
22-5, 24–26	394.74	149.9	66.0	3.900	150	15.3	56.1	2.021	N
22-5, 55–57	395.05	207.2	76.8	4.978	200	194.4	52.3	0.200	N
23-1, 23–25	398.23	18.3	58.9	14.204	150	57.7	57.3	3.935	N
23-2, 140–143	400.90	24.3	56.2	11.201	150	65.0	63.9	1.698	N
23-3, 12–15	401.12	236.9	60.1	17.074	150	266.8	26.6	3.494	N
23-3, 145–147	402.45	356.7	40.3	5.741	100	2.9	10.4	0.066	N
23-4, 7–10	402.57	20.5	49.8	18.407	100	54.5	36.6	4.848	N
23-4, 115–117	403.65	293.0	41.7	5.282	150	305.0	−3.4	3.561	R
23-5, 3–6	404.13	204.8	32.1	13.563	200	213.8	−5.2	6.519	R
25-5, 135–138	405.35	25.8	77.1	6.713	200	285.8	−37.4	2.165	R
24-1, 9–12	407.59	337.7	−27.7	2.538	100	320.3	−62.2		N
24-1, 144–147	408.94	339.6	50.3	5.047	100	348.1	49.5	4.417	N
24-2, 5–8	409.05	224.5	46.9	5.383	100	220.0	48.7	3.719	N
24-3, 7–10	410.57	294.8	57.2	3.790	100	288.6	52.6	1.877	N
25-1, 55–58	417.55	121.3	62.2	15.832	100	127.4	55.6	3.988	N
25-2, 5–8	418.55	308.5	57.2	28.718	100	284.7	61.5	3.144	N
26-1, 21–24	426.71	265.0	42.6	0.485	100	274.5	28.3	0.180	N
27-1, 7–10	436.07	353.2	−0.2	1.395	100	305.0	1.3	0.752	R?
28-1, 36–39	445.86	302.9	64.1	6.923	100	295.2	46.3	2.388	N
28-1, 101–103	448.01	336.0	54.5	97.37	100	328.4	43.8	24.589	N
28-3, 35–38	448.85	171.7	60.3	62.027	100	177.3	52.7	27.195	N
29-1, 5–8	455.05	173.7	58.1	54.863	100	175.6	46.5	22.540	N
35-1, 75–77	512.75	129.9	45.2	0.354	NRM				N
36-1, 5–7	521.55	316.1	50.9	0.148	NRM				N
37-1, 41–43	522.91	124.6	23.3	0.972	100	120.0	44.2	0.862	N
37-1, 106–108	523.56	224.3	49.5	0.503	100	218.1	53.0	0.280	N
37-2, 4–7	524.04	63.3	−38.7	0.451	50	70.8	−48.1	0.196	R
38-1, 35–38	531.55	181.7	−63.6	0.154	100	302.0	−30.0	0.152	R
39-1, 24–27	540.74	277.3	36.5	0.020	NRM				N
40-1, 22–25	550.22	89.3	53.0	0.092	NRM				N
42-1, 52–55	569.52	271.5	61.4	0.125	NRM				N
42-2, 12–15	570.62	139.6	4.9	0.218	50	116.4	24.2	0.206	N
42-3, 13–16	571.13	22.1	17.9	0.327	50	358.8	65.1	0.424	N
43-1, 92–94	579.42	328.9	60.7	0.824	50	343.2	57.4	0.526	N
43-2, 29–31	580.29	22.7	59.5	0.640	50	1.0	47.9	0.633	N
43-3, 45–47	581.95	102.8	51.4	1.110	50	105.8	57.4	0.716	N
43-4, 68–70	583.63	148.7	50.7	1.288	50	151.0	48.0	1.452	N
44-1, 32–34	588.32	183.0	59.9	0.234	50	182.9	49.1	0.521	N
44-2, 53–55	590.03	222.4	59.2	0.813	50	203.5	57.7	0.874	N
44-3, 4–6	591.04	317.0	51.4	0.550	50	306.1	55.4	0.391	N
44-4, 121–123	593.71	230.7	62.1	1.280	50	231.9	53.7	1.231	N
45-1, 67–69	598.17	254.9	52.3	1.564	50	257.1	45.6	1.646	N
45-2, 7–9	599.07	82.7	52.0	1.103	50	82.8	48.3	1.127	N
45-3, 15–17	600.65	235.7	50.0	1.663	50	234.6	53.6	1.654	N
45-4, 40–42	602.40	262.8	51.4	1.743	50	253.1	51.6	1.561	N
45-5, 15–17	603.65	182.7	55.5	1.649	50	186.8	54.3	1.330	N
46-1, 59–61	607.59	97.1	50.7	4.272	50	103.3	65.5	1.773	N
46-2, 62–64	609.12	105.4	49.9	2.237	50	107.7	41.6	1.612	N
46-3, 51–53	610.51	70.8	58.7	2.147	50	71.5	52.5	2.105	N
46-4, 66–68	612.16	74.2	58.2	2.042	50	71.6	60.6	2.188	N
47-1, 110–112	617.60	83.3	67.9	5.725	50	85.2	58.2	1.800	N
47-2, 20–22	618.20	4.5	49.8	1.401	50	350.4	42.2	1.321	N
47-3, 53–55	620.03	206.4	54.0	1.721	50	225.0	53.6	1.450	N
47-4, 10–12	621.10	63.7	65.1	0.943	50	67.5	59.1	0.997	N
47-4, 97–99	621.97	203.2	65.1	1.453	200	205.1	51.9	0.900	N
47-5, 16–18	622.66	156.3	61.3	2.535	200	158.3	50.0	1.559	N
48-1, 15–17	626.15	161.9	−61.3	1.826	50	226.2	−53.4	1.317	R
52-1, 27–29	664.27	325.6	−1.6	0.760	75	290.2	41.7	0.837	N
54-1, 12–14	683.12	2.2	63.2	4.419	75	358.5	58.3	4.911	N
54-2, 80–82	685.30	93.3	64.0	2.821	75	95.3	54.0	2.657	N
54-3, 109–111	687.09	66.8	57.6	1.119	50	52.4	−52.4	1.042	N
54-4, 32–34	687.82	274.2	72.0	1.353	50	263.2	74.9	0.790	N
55-1, 29–31	692.29	3.8	55.6	0.674	50	359.9	45.7	0.553	N
55-2, 16–18	693.66	103.3	56.3	1.263	50	111.0	56.0	1.907	N
55-3, 135–137	696.35	337.2	55.9	18.036	50	332.1	56.0	13.896	N
55-4, 67–69	697.17	29.9	51.1	10.214	50	44.3	47.0	8.803	N
55-5, 75–77	698.75	295.6	64.3	1.586	100	295.0	46.1	1.385	N
56-1, 139–141	702.39	177.8	77.6	2.161	100	183.3	68.2	1.612	N
56-2, 49–51	702.99	245.5	52.9	2.816	100	245.0	55.0	1.450	N
56-3, 91–93	704.91	8.7	53.0	20.059	100	7.9	56.1	11.317	N
56-4, 35–37	705.85	308.4	70.6	1.804	100	307.1	59.4	0.894	N
56-5, 30–32	707.30	348.0	54.2	16.428	100	345.3	56.6	8.623	N
57-1, 22–24	710.22	195.7	71.3	22.861	100	167.8	57.1	12.273	N
57-2, 22–25	711.75	299.1	51.2	16.844	100	290.5	45.7	10.711	N
57-3, 24–26	713.24	214.7	59.1	40.611	100	205.4	56.1	28.791	N
57-4, 52–54	716.02	92.9	52.2	19.362	100	94.3	52.7	7.371	N
57-5, 8–10	717.08	149.9	60.5	8.972	100	155.2	64.0	6.411	N
58-1, 107–109	720.07	121.6	63.6	38.502	100	133.6	62.3	22.985	N
58-2, 18–20	620.68	245.2	55.7	69.032	100	240.2	52.1	42.801	N
58-3, 45–47	722.45	23.0	53.0	35.461	100	26.6	45.8	19.008	N

Table 3. (Continued).

Core-Sample (interval in cm)	Sub-bottom depth (m)	Before demagnetization D (°)	Before demagnetization I (°)	Before demagnetization Int (μG)	Demagnetization field (Oe)	After demagnetization D (°)	After demagnetization I (°)	After demagnetization Int (μG)	Polarity
Hole 549 (Cont.)									
58-4, 22-24	723.72	280.3	57.6	80.158	100	277.8	53.3	54.604	N
58-5, 19-22	725.19	254.3	60.1	10.078	100	251.3	56.4	4.324	N
58-6, 19-21	725.69	103.4	47.9	113.185	100	105.6	45.8	76.069	N
58-7, 15-17	728.	275.3	44.6	87.493	100	268.6	43.8	58.705	N
59-1, 16-18	728.16	328.8	56.1	62.597	100	323.6	52.5	30.187	N
59-2, 16-17	729.66	13.5	71.3	3.235	100	13.3	53.4	0.545	N
59-3, 11-13	731.11	141.0	59.5	76.498	100	150.1	63.2	19.118	N
60-1, 109-111	738.09	150.6	56.6	2.018	100	152.7	51.7	1.061	N
60-2, 98-100	739.98	39.5	60.6	1.310	100	83.5	63.1	0.631	N
60-3, 33-35	740.33	115.3	64.8	1.999	100	95.9	60.8	1.882	N
60-4, 36-38	741.86	244.9	59.5	4.092	100	259.0	72.6	1.632	N
60-5, 31-33	743.31	21.0	53.8	27.247	100	23.0	51.7	14.311	N
60-6, 37-39	745.87	288.6	51.6	13.822	100	289.1	51.7	5.552	N
61-1, 25-27	746.25	96.9	66.3	0.230	100	17.9	70.1	0.327	N
61-2, 49-51	747.99	351.1	55.1	1.780	100	340.9	53.7	1.207	N
61-3, 16-18	749.16	342.6	53.6	0.603	100	312.6	48.4	1.115	N
73-1, 95-97	807.45	94.2	48.9	0.347	50	81.9	53.9	0.775	N
73-2, 87-89	808.87	236.1	47.0	1.934	50	226.9	60.0	1.659	N
74-1, 14-17	811.14	264.2	61.3	1.535	50	246.6	56.9	0.989	N
74-2, 43-45	812.93	232.9	55.5	1.242	100	234.4	53.5	1.584	N
74-3, 121-124	815.21	233.4	58.6	0.768	100	211.7	58.4	0.512	N
75-1, 128-131	817.25	156.4	61.9	1.414	100	167.0	58.8	1.225	N
75-2, 124-126	818.74	313.8	68.2	0.633	100	200.4	76.9	0.336	N
75-3, 7-10	819.07	67.0	75.3	0.337	100	64.0	32.2	0.113	N
76-1, 102-104	826.02	19.6	61.0	5.593	100	15.7	62.0	2.792	N
76-2, 134-136	827.84	306.5	72.5	4.449	100	308.9	66.4	2.180	N
76-3, 7-9	828.07	291.4	77.4	2.572	100	294.5	60.9	2.265	N
78-1, 86-88	843.86	344.7	59.7	12.276	100	347.4	55.5	7.478	N
79-1, 61-63	852.61	146.6	62.5	2.776	100	151.8	58.2	2.610	N
80-1, 64-65	861.64	174.2	54.5	0.951	50	162.9	59.8	1.359	N
80-2, 79-81	863.29	100.6	22.1	0.808	50	104.1	20.6	0.763	N
81-1, 135-137	871.35	147.2	65.6	2.090	50	152.0	54.8	1.385	N
81-2, 44-46	871.94	271.8	51.2	0.548	50	262.9	54.1	0.535	N
82-1, 33-35	874.83	323.4	42.4	0.293	50	11.0	68.2	0.323	N
82-2, 51-54	875.01	279.1	−15.3	0.401	150	261.4	−1.5	0.335	R?
83-1, 13-15	879.13	216.2	66.6	0.125	100	230.8	51.8	0.207	N
83-2, 69-71	881.19	248.3	84.3	1.327	50	229.1	79.4	1.237	N
83-3, 9-11	882.09	290.3	−59.6	0.496	75	273.6	−65.0	0.083	R
84-1, 56-59	884.56	149.2	72.4	0.863	150	151.0	62.2	0.772	N
84-2, 82-84	886.32	71.3	28.1	1.584	300	66.7	34.0	1.339	N
85-1, 19-21	888.19	219.9	56.4	3.415	100	221.2	54.5	2.032	N
85-2, 49-51	889.97	118.7	54.3	1.197	100	136.0	55.6	0.673	N
85-3, 9-11	891.09	231.2	58.6	2.858	100	240.8	50.9	1.897	N
86-1, 16-18	897.16	209.3	67.4	0.619	100	166.5	47.5	0.354	N
86-2, 27-29	898.77	211.0	76.2	0.259	25	140.5	76.8	0.205	N
86-3, 25-27	900.25	178.2	47.0	0.095	25	228.1	60.6	0.175	N
87-2, 37-39	907.37	224.9	53.5	4.133	50	234.1	58.1	4.229	N
87-3, 9-11	909.9	11.8	56.9	1.272	50	9.2	55.2	1.222	N
88-1, 22-25	910.72	179.9	52.3	2.017	50	177.7	53.9	1.551	N
88-2, 99-102	912.99	245.3	60.2	0.082	NRM				N
88-3, 37-40	913.87	252.1	69.1	0.118	100	186.2	63.4	0.277	N
89-1, 88-91	920.38	138.2	56.5	1.290	100	137.6	51.9	0.663	N
89-2, 128-131	922.28	352.5	56.9	0.657	50	353.0	51.4	0.691	N
90-1, 55-57	929.05	267.8	−2.6	1.409	75	279.0	33.3	0.395	N?
90-2, 33-35	930.33	320.9	44.3	1.010	50	340.6	61.2	0.942	N
90-3, 41-43	931.91	357.8	60.8	2.191	50	2.6	63.4	0.359	N
91-1, 57-60	938.07	87.7	72.7	0.064	NRM				N
91-2, 41-43	939.41	355.0	63.1	0.139	50	355.8	69.6	0.35	N
92-1, 50-52	947.0	281.6	43.9	0.046	NRM				N
93-1, 46-48	955.96	305.8	23.6	0.280	50	314.5	47.3	0.338	N
94-1, 20-22	964.70	80.3	12.4	0.176	50	108.6	68.4	0.676	N

Note: Symbols and abbreviations as in Table 1.

The paleomagnetic data show no evidence of hiatuses in the Upper Cretaceous to Paleocene section of Hole 550B, but biostratigraphic studies suggest that the lower part of Anomaly 33 and the upper part of the long Cretaceous normal polarity interval may be absent. Three short reversals have been detected in Cores 23 to 25 that may represent the mixed polarity interval of late Albian age identified by van Hinte (1976) and recognized at DSDP Site 263 off Western Australia (Green and Brecher, 1974 and Jarrard, 1974) and Sites 400 and 402 in the Bay of Biscay (Hailwood, 1979). The identification of these reversals in the sediments directly overlying basement is of particular significance in view of the age of the oldest sediments at this site. The paleomagnetic evidence therefore suggests a late Albian age for these sediments. This is in broad agreement with the biostratigraphic studies.

Site 551

Site 551 was washed to 100 m and then rotary drilled. The sediments recovered were a condensed sequence of early Eocene calcareous muds resting uncomfortably on Late Cretaceous nannofossil chalks. The results from this hole are listed in Table 5. Figure 18 shows the downhole variation in inclination and the polarity reversal sequence deduced for the hole. Three normal polarity intervals occur in the Cretaceous part of the sequence. The upper two, above the Cenomanian/Campanian unconformity, probably represent Anomalies 32 and 33, the lowest one Anomaly 34.

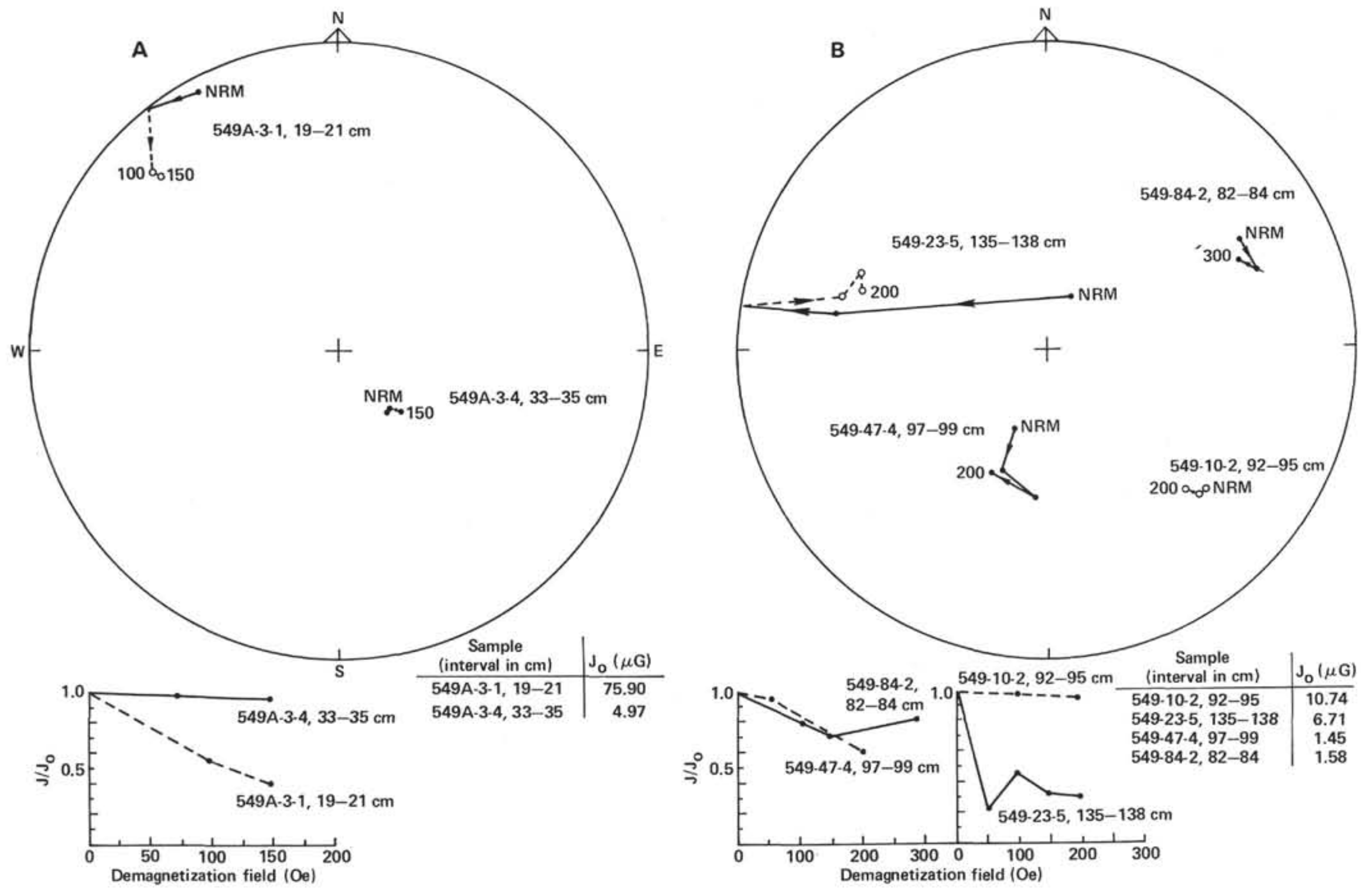

Figure 9. Response of typical samples from Site 549 to af demagnetization. A. Samples from Hole 549A. B. Samples from Hole 549. Symbols as in Fig. 2.

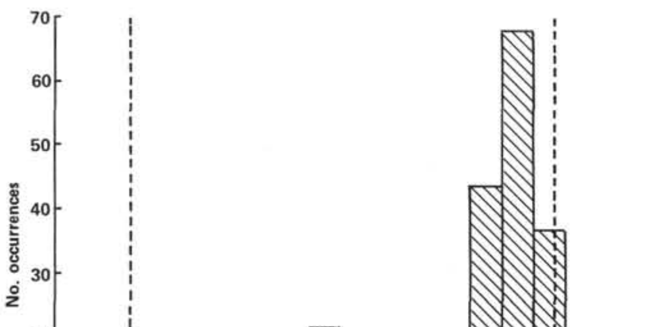

Figure 10. Histogram of magnetic inclination values for Hole 549. Dashed lines represent present-day theoretical geocentric dipole values.

CONCLUSIONS

Magnetostratigraphic studies for the sites drilled across the Goban Spur have enabled polarity reversal sequences to be established. The correlation of reversal sequences with standard Cenozoic and Cretaceous polarity time scales permits the refinement and enhancement of the biostratigraphic dating of the sediments.

In this study Site 549 provided the section most suitable for paleomagnetic studies, because an almost complete sequence of upper Paleocene to upper Oligocene pelagic sediments containing rich faunal assemblages was recovered. Unfortunately, the upper Eocene and Oligocene sediments were too weakly magnetized for an unequivocal magnetostratigraphy to be determined, but good results were obtained from the middle Eocene and upper Paleocene section. Figure 19 shows a summary of the paleomagnetic and biostratigraphic data for Sites 548, 549, and 550, together with a magnetostratigraphic correlation. Although the section at Site 549 appeared to be complete from biostratigraphic evidence, studies of the ash layers (Knox, this volume) indicate a hiatus at the NP9/NP10 boundary. The normal polarity interval at the NP9/NP8 boundary at Site 549 is rather low to be Anomaly 25, which may be absent as a result of the hiatus. If it is absent, the correlation shown in Figure 19 between the normal polarity intervals assigned to Anomaly 25 at Sites 549 and 550 would be incorrect.

Figure 19 also illustrates generally better agreement between the magnetostratigraphy and the nannoplankton zones than the foraminifer zones. For example, the

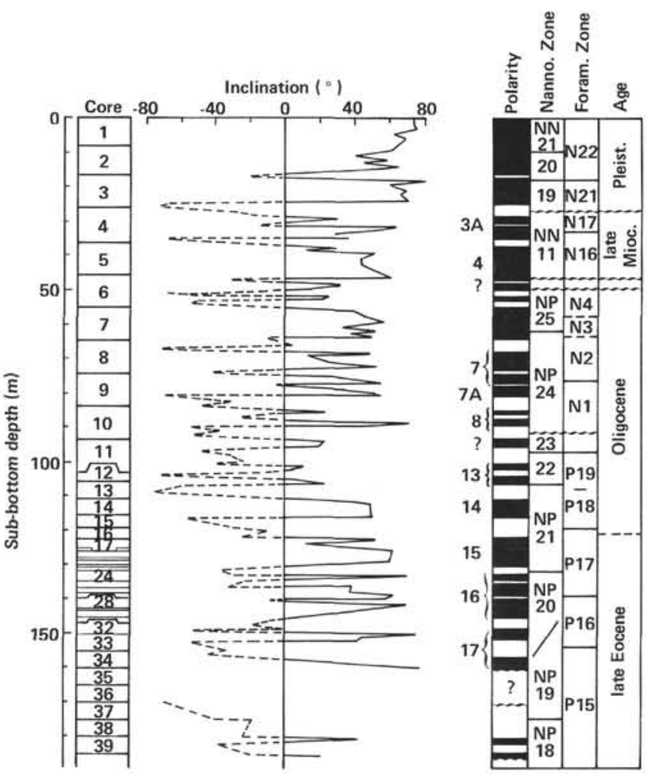

Figure 11. Downhole variation of magnetic inclination and inferred polarity reversal sequence for Hole 549A.

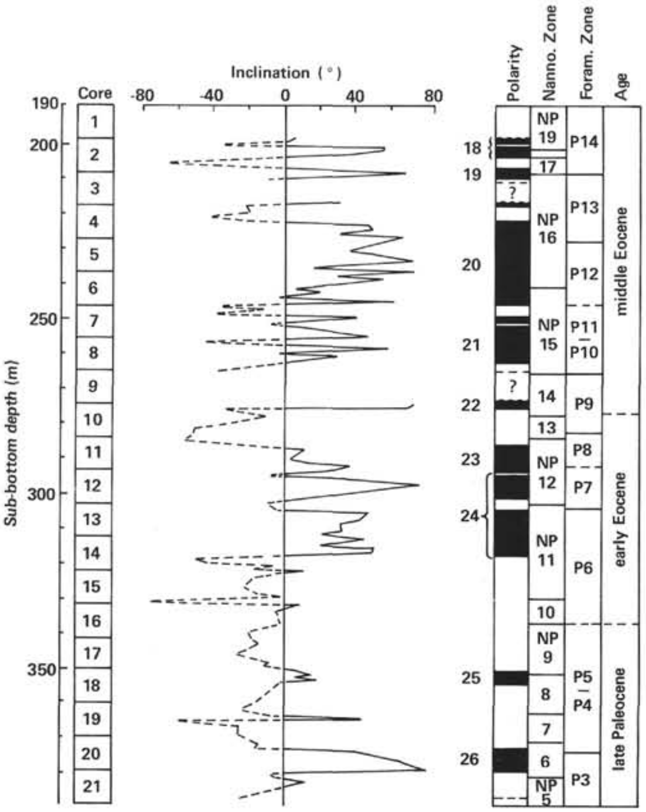

Figure 12. Variation of magnetic inclination with depth and inferred polarity reversal sequence for the late Paleocene to middle Eocene sediments from Hole 549.

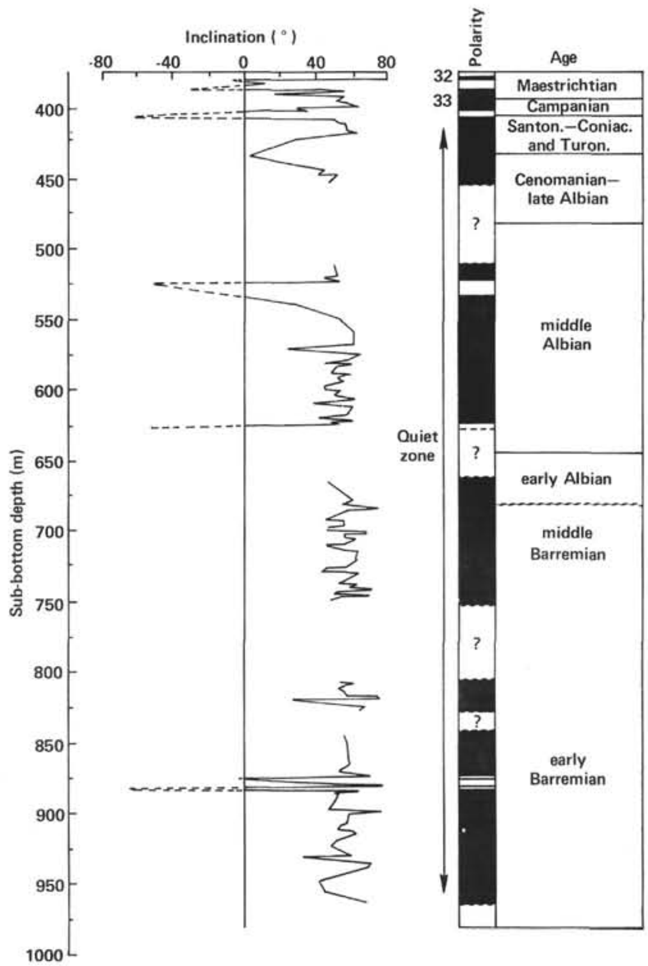

Figure 13. Downhole variation of magnetic inclination and inferred polarity reversal sequence for the Cretaceous sediments from Hole 549.

normal polarity interval assigned to Anomaly 23 lies within NP12 at both Sites 549 and 550, but it lies within P8/P7 at Site 549 and P9/P8 at Site 550.

An important result of the paleomagnetic studies is that changes in the values of NRM intensity and magnetic susceptibility correlated with changes in these values at other sites. At Sites 548 and 549 a significant downhole increase in the values of NRM intensity and magnetic susceptibility was noted in nannoplankton Zone NP14, which agrees with the results from Holes 400A and 401 of Leg 48. This increase is of particular interest in view of the results of the magnetic fabric studies on these sediments (Hailwood and Folami, this volume), which suggest that a change in sediment transport processes occurred at this time.

The paleomagnetic studies are also of value in assigning absolute ages to the sediments. The assignment of absolute ages is dealt with in Snyder et al. (this volume).

ACKNOWLEDGMENTS

I would like to thank all the people who have assisted me during the course of this research, particularly Ernie Hailwood for his helpful advice and encouragement. I am grateful to the shipboard scientific and technical party, especially to Carla Müller and Scott Snyder for access to their paleontological results.

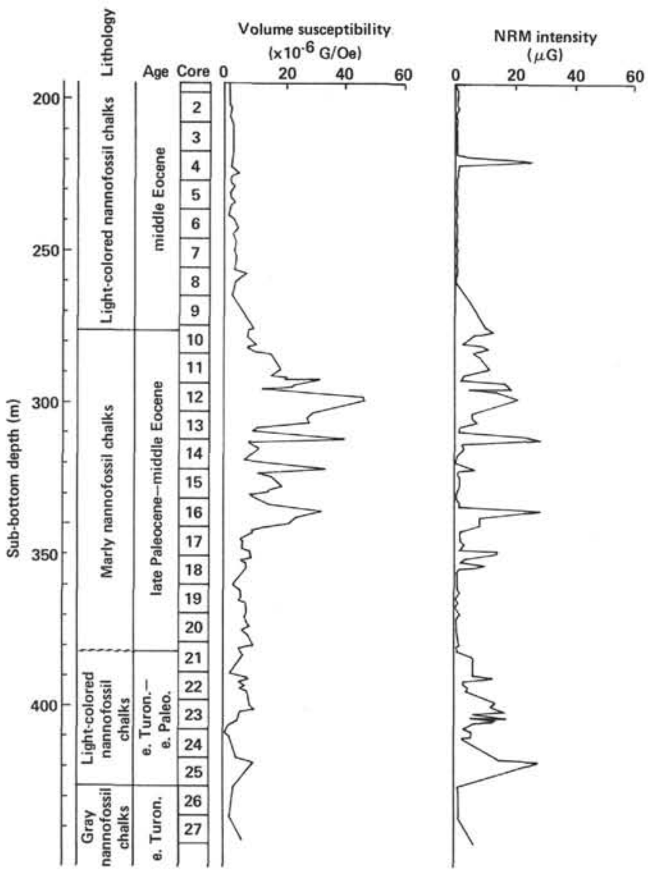

Figure 14. Downhole variation of magnetic susceptibility and NRM intensity, Hole 549.

I would like to thank Joan Wedge and Jean Watson for typing this manuscript. Financial assistance from the Natural Environment Research Council is gratefully acknowledged.

REFERENCES

Green, K. A., and Brecher, A., 1974. Preliminary paleomagnetic results for sediments from Site 263, Leg 27. *In* Veevers, J. J., Heirtzler, J. R., et al., *Init. Repts. DSDP*, 27: Washington (U.S. Govt. Printing Office), 405–413.

Hailwood, E. A., 1979. Paleomagnetism of late Mesozoic to Holocene sediments from the Bay of Biscay and Rockall Plateau, drilled on IPOD Leg 48. *In* Montadert, L., Roberts, D. G., et al., *Init. Repts. DSDP*, 48: Washington (U.S. Govt. Printing Office), 305–339.

Hailwood, E. A., Bock, W., Costa, L., Dupeuble, P. A., Müller, C., and Schnitker, D., 1979. Chronology and biostratigraphy of Northeast Atlantic sediments, DSDP Leg 48. *In* Montadert, L., Roberts, D. G., et al., *Init. Repts. DSDP*, 48: Washington (U.S. Govt. Printing Office), 1119–1141.

Jarrard, R. D., 1974. Paleomagnetism of some Leg 27 sediment cores. *In* Veevers, J. J., Heirtzler, J. R., et al., *Init. Repts. DSDP*, 27: Washington (U.S. Govt. Printing Office), 415–423.

LaBrecque, J. L., Kent, D. V., and Cande, S. C., 1977. Revised magnetic polarity time scale for the Late Cretaceous and Cenozoic time. *Geology*, 5:330–335.

Lowrie, W., and Alvarez, W., 1981. One hundred million years of geomagnetic polarity history. *Geology*, 9:392–397.

Molyneux, L., 1971. A complete results magnetometer for measuring the remanent magnetization of rocks. *Geophys. J. R. Astron. Soc.*, 24:429–433.

Ness, G., Levi, S., and Couch, R., 1980. Marine magnetic anomaly time scales for the Cenozoic and Late Cretaceous. A précis, critique and synthesis. *Rev. Geophys. Space Phys.*, 18:753–770.

van Hinte, J. E., 1976. A Cretaceous time scale. *Bull. Am. Assoc. Pet. Geol.*, 60:498–516.

Date of Initial Receipt: February 14, 1983
Date of Acceptance: June 22, 1983

Table 4. Paleomagnetic results, Site 550.

Core-Sample (interval in cm)	Sub-bottom depth (m)	Before demagnetization D (°)	Before demagnetization I (°)	Before demagnetization Int (μG)	Demagnetization field (Oe)	After demagnetization D (°)	After demagnetization I (°)	After demagnetization Int (μG)	Polarity
Hole 550									
5-1, 26–28	128.26	136.8	11.8	0.158	25	155.5	62.7	0.204	N
5-1, 124–127	129.24	28.5	−45.2	0.035	NRM				R
5-2, 26–28	129.76	342.4	−19.0	36.836	50	340.0	−19.1	33.628	R
5-2, 111–113	130.61	305.8	07.3	0.713	50	300.1	−11.6	0.638	R
5-3, 23–29	131.27	5.0	1.9	0.004	NRM				?
5-3, 112–114	132.12	198.4	58.3	1.975	50	184.4	68.4	3.080	N
5-4, 27–29	132.77	259.2	−67.0	0.066	NRM				R
5-4, 113–115	133.63	82.8	19.2	0.108	NRM				N
5-5, 31–33	134.31	175.0	−9.8	0.093	NRM				R
5-6, 33–35	135.83	162.4	−0.3	0.071	NRM				R
5-7, 31–33	137.31	340.1	−33.6	0.085	NRM				R
6-1, 31–33	137.81	82.2	−21.0	1.126	50	62.0	−19.5	0.608	R
6-2, 35–37	139.35	145.1	42.0	0.121	25	222.4	−79.5	0.093	R
6-3, 139–141	141.89	240.4	−42.3	0.548	25	213.9	−35.1	0.400	R
6-4, 34–36	142.34	113.4	−15.3	0.198	25	146.3	25.6	0.254	N
6-5, 11–13	143.61	2.9	34.1	0.093	NRM				N
6-6, 129–131	146.29	281.4	62.2	0.113	25	267.5	70.9	0.098	N
6-7, 37–39	146.87	12.9	−1.9	0.315	25	259.9	60.3	0.023	N
7-1, 29–31	147.29	82.9	43.8	4.337	50	80.0	43.0	3.977	R
7-3, 124–126	151.24	302.9	−49.0	0.096	NRM				R
7-4, 18–20	151.68	323.4	−47.0	2.321	50	329.7	−49.0	2.398	R
7-5, 126–128	154.26	140.8	7.5	0.124	25	61.9	−48.1	0.05	R
7-6, 26–28	154.76	50.0	55.9	0.114	NRM				N
8-3, 124–126	160.74	349.3	9.9	0.041	NRM				?
8-4, 56–58	161.56	136.6	−18.9	0.221	25	87.6	−74.3	0.107	R
8-5, 21–23	162.71	147.2	−9.0	0.092	NRM				R
9-1, 73–75	166.73	178.2	36.7	0.140	NRM				N
9-3, 18–20	169.18	11.8	2.2	0.381	25	14.6	−16.6	0.387	R
9-4, 67–69	171.17	137.3	19.3	0.101	NRM				N?
9-5, 7–9	172.07	59.8	56.4	0.129	NRM				N
9-6, 16–18	173.66	104.5	28.3	0.081	NRM				N
9-6, 127–129	174.77	275.9	21.9	0.032	NRM				N
10-1, 134–136	176.84	21.5	−34.3	0.103	NRM				R
10-2, 111–113	178.11	238.5	−44.6	0.120	NRM				R
10-3, 41–43	178.91	23.5	34.6	0.453	25	40.2	26.3	0.319	N
11-1, 23–25	185.23	84.2	−46.8	0.168	25	104.2	−13.6	0.255	R
11-2, 53–55	187.03	83.2	−22.3	0.178	25	127.9	−56.2	0.204	R
11-3, 99–101	188.99	339.9	−48.6	0.840	25	309.3	−61.4	0.939	R
12-3, 37–39	197.87	249.3	−43.0	1.773	50	247.6	−27.1	1.335	R
12-4, 25–27	199.25	205.7	8.5	0.163	25	191.2	−14.8	0.297	R
13-1, 24–26	204.22	111.7	−38.9	0.112	NRM				R
14-1, 37–39	213.87	53.0	−54.0	0.091	NRM				R
14-2, 43–45	215.43	80.6	54.6	0.180	25	335.5	−16.7	0.060	R
14-3, 31–33	216.81	330.0	−57.6	0.236	25	16.8	−13.6	0.066	R
14-3, 106–108	217.56	231.0	−58.0	0.024	NRM				R
15-1, 27–29	223.27	298.3	7.3	0.047	NRM				?
15-1, 77–79	223.37	347.0	2.1	0.009	NRM				R
16-1, 19–21	232.69	348.9	6.8	0.153	25	32.3	−13.3	0.141	R
16-2, 18–20	234.18	106.3	4.8	0.203	25	94.0	−8.7	0.150	R
16-2, 91–93	234.91	38.8	46.8	0.060	NRM				N?
16-3, 23–25	235.73	342.1	−76.4	0.280	25	140.4	62.9	0.193	N
16-3, 95–97	236.45	0.0	16.8	1.948	50	30.5	18.8	0.905	N
16-4, 14–16	237.14	35.3	13.9	16.433	50	35.3	9.2	14.94	N
17-1, 131–133	243.31	19.0	38.7	2.987	50	8.3	43.8	2.567	N
17-2, 20–22	243.70	256.7	15.1	4.000	50	253.0	22.3	3.776	N
17-3, 28–30	245.28	92.7	18.3	4.308	50	100.0	18.8	4.196	N
18-1, 43–45	251.93	20.6	−27.1	0.410	25	12.3	−22.1	0.139	R
18-2, 25–27	253.25	13.8	−47.4	0.159	NRM				R
18-3, 24–26	254.74	108.4	−15.3	0.122	NRM				R
18-4, 8–10	256.08	18.6	−21.1	0.103	NRM				R
19-1, 29–31	261.29	340.4	−11.9	0.152	25	163.0	−31.6	0.096	R
19-1, 96–98	261.96	306.0	−36.9	0.160	NRM				R
19-2, 17–20	262.67	6.2	7.0	0.430	25	22.1	−2.7	0.544	R
19-3, 5–8	264.05	17.2	−25.5	0.155	NRM				R
20-11, 6–8	279.80	96.1	−2.8	13.797	50	100.9	−1.9	11.037	R
21-1, 19–21	280.19	101.3	25.9	0.027	NRM				N
21-2, 40–42	281.90								
21-2, 108–110	282.58	257.8	−32.8	0.180	NRM				R
21-3, 28–30	283.28	29.2	−24.5	0.017	NRM				R
22-1, 58–60	290.08	252.7	−61.2	1.743	50	248.6	−56.7	1.716	R
22-1, 131–133	290.81	121.9	63.8	4.460	200	155.7	−44.1	1.443	R
22-2, 51–53	291.51	147.9	74.1	5.468	50	75.0	77.0	0.279	N
22-2, 113–115	292.13	185.0	66.0	3.347	50	177.0	40.5	0.216	N
22-3, 58–60	293.08	242.4	77.7	12.300	50	355.7	54.7	0.444	N
22-4, 58–60	294.58	191.4	80.1	14.949	50	192.6	71.1	1.618	N
22-5, 28–30	295.78	23.5	77.5	3.389	50	195.8	76.8	0.145	N
23-1, 118–120	200.18	48.8	−44.8	0.869	25	43.3	−47.4	1.040	R
23-2, 83–85	301.33	255.9	62.4	10.684	50	253.1	63.5	2.358	N
23-3, 77–79	302.77	120.0	53.4	21.867	50	120.0	41.8	13.035	
23-4, 123–125	304.73	332.9	87.2	2.373	50	40.4	−49.6	2.060	R
23-5, 84–86	305.84	125.1	67.9	17.333	50	139.3	68.1	4.607	N
23-11, 17–19	308.17	222.4	−79.0	0.742	50	345.7	−78.8	0.342	R
24-1, 5–6	308.55	260.1	57.4	28.710	50	249.9	53.0	14.965	N
24-1, 106–108	309.56	311.6	41,1	28.189	200	316.3	29.7	9.875	N
24-2, 4–6	310.04	48.5	72.1	18.176	75	273.9	−48.0	4.144	R
24-2, 136–138	311.36	69.3	62.1	20.634	200	187.5	−5.8	3.049	R
24-3, 29–31	311.79	75.7	59.6	20.783	150	137.4	53.0	5.632	N
24-3, 123–125	312.73	346.6	45.4	27.164	150	8.5	−24.7	8.859	R

Table 4. (Continued).

Core-Sample (interval in cm)	Sub-bottom depth (m)	Before demagnetization D (°)	Before demagnetization I (°)	Before demagnetization Int (μG)	Demagnetization field (Oe)	After demagnetization D (°)	After demagnetization I (°)	After demagnetization Int (μG)	Polarity
Hole 550 (Cont.)									
24-4, 66–68	313.66	333.2	71.2	12.634	75	61.3	−31.1	3.494	R
24-4, 121–123	314.21	339.9	32.4	15.287	150	194.9	−37.0	10.084	R
24-5, 45–47	314.95	326.7	57.4	21.135	100	210.6	−49.6	4.358	R
24-5, 101–103	315.51	317.9	54.2	26.673	150	284.9	48.6	6.976	N
25-1, 69–71	318.69	97.3	56.8	29.252	200	128.1	37.1	6.785	N
25-1, 128–130	319.28	38.0	39.2	11.872	150	44.6	−45.4	13.151	R
25-2, 6–8	319.56	28.8	59.6	18.703	100	0.7	−38.2	10.248	R
25-3, 84–86	321.84	296.7	50.4	15.785	100	46.7	−0.5	6.492	R
25-4, 16–18	433.66	135.1	78.1	17.366	100	157.3	−1.5	13.143	R
25-5, 15–17	324.15	37.4	50.0	13.666	100	7.8	−22.5	15.852	R
26-1, 17–19	327.67	304.9	41.7	42.004	400	259.4	46.3	0.534	N
26-1, 124–126	328.74	326.3	37.8	38.100	150	329.0	37.1	18.275	N
27-1, 33–36	337.33	255.3	−0.2	29.273	150	243.5	−36.6	36.07	R
27-2, 28–31	338.78	348.5	−29.6	32.426	150	347.9	−36.7	30.535	R
27-3, 23–26	340.23	51.7	9.1	32.547	150	57.5	−32.7	27.093	R
27-3, 146–149	341.46	296.0	−25.4	23.348	150	277.8	−33.6	18.559	R
27-4, 117–120	342.67	143.8	50.9	58.304	150	150.6	40.4	28.385	N
27-5, 20–23	343.20	295.4	48.2	31.351	150	42.0	0.3		N
27-6, 12–15	344.6	311.8	39.8	29.348	150	311.4	34.9	23.927	N
27-6, 102–105	345.02	45.8	−50.5	32.826	150	45.6	−54.5	14.846	R
27-7, 16–18	346.16	229.1	−29.2	22.234	150	222.8	−33.9	19.856	R
28-1, 44–47	346.94	345.6	29.3	33.882	150	345.8	26.6	25.857	N?
28-1, 112–114	347.62	298.7	−20.4	25.41	150	297.6	−22.1	21.319	R
28-2, 26–29	348.26	290.3	−2.0	12.312	150	288.6	−7.3	10.587	R
28-2, 138–140	349.38	68.1	−12.1	19.236	150	72.9	−14.1	17.529	R
28-3, 36–38	349.86	318.1	52.6	18.716	150	321.2	46.8	11.981	N
28-4, 32–34	351.32	183.5	48.7	21.840	150	182.1	49.4	18.844	N
28-5, 24–26	352.34	136.2	56.0	29.927	150	139.4	53.4	22.107	N
29-1, 15–18	356.15	97.2	49.5	37.912	150	96.7	43.0	18.00	N
29-2, 26–29	357.76	268.5	41.7	46.888	150	270.2	37.6	25.018	N
29-3, 27–30	359.27	107.3	56.9	35.857	150	47.5	19.9		N
29-3, 103–105	360.03	174.0	−9.8	19.240	150	196.8	−30.1	7.941	R
29-4, 29–32	360.79	149.4	20.4	13.074	150	141.9	−8.9	11.945	R
29-5, 17–20	362.17	341.4	12.7	12.820	150	335.6	−32.9	19.393	R
29-6, 38–41	363.88	137.7	28.2	12.221	150	149.4	−25.0	20.549	R
30-1, 11–14	365.61	36.2	2.6	18.888	150	357.8	−61.0	15.080	R
30-1, 88–91	366.38	134.3	−37.3	9.877	150	138.6	−27.6	5.221	R
30-2, 2–5	367.02	58.9	61.6	10.072	150	18.2	53.3	2.190	N?
30-3, 32–35	368.82	103.7	−2.1	0.350	50	168.0	−31.8	0.017	R
30-4, 10–13	370.10	337.8	82.5	3.867	50	194.7	−9.4	0.811	R
30-5, 14–17	371.64	217.2	21.7	8.740	50	221.7	−24.0	14.209	R
30-6, 14–17	373.14	246.1	−3.2	8.306	150	249.9	−39.6	12.546	R
31-1, 18–21	375.18	63.5	−14.9	6.161	150	59.9	−47.9	12.603	R
31-2, 29–31	376.87	118.6	49.1	13.327	150	85.3	−17.9	9.997	R
31-3, 29–32	378.29	135.1	10.7	20.395	150	149.3	−24.4	23.965	R
31-4, 32–34	379.82	273.3	5.1	21.749	150	264.3	−13.4	19.576	R
31-5, 26–28	381.26	90.8	−0.7	0.438	50	68.5	−64.4	5.624	R
32-1, 14–16	384.64	29.5	65.1	9.430	50	111.4	36.7	1.652	N?
32-2, 31–33	386.31	321.5	−22.4	6.914	150	307.7	−37.3	9.816	R
32-3, 24–26	387.74	207.6	8.8	17.064	150	202.8	−32.6	24.53	R
32-4, 27–29	389.27	58.4	28.0	4.181	150	69.9	−39.4	7.364	R
32-5, 21–23	390.71	121.1	17.4	13.186	150	123.3	−27.4	17.917	R
32-6, 45–47	392.45	4.1	−4.4	21.919	150	0.1	−34.8	25.48	R
32-7, 37–39	393.87	42.1	23.1	13.894	150	53.8	−20.3	14.281	R
33-1, 16–18	394.16	151.1	30.8	2.717	150	161.6	−36.6	3.512	R
33-2, 23–25	395.73	39.9	55.4	11.332	150	43.3	−36.6	7.169	R
33-2, 129–131	396.79	342.5	−0.0	10.909	150	352.1	−29.3	11.397	R
33-3, 19–21	397.19	93.2	58.0	18.371	150	98.1	−22.3	22.487	R
33-4, 24–26	398.74	99.3	88.8	18.682	150	269.5	−26.0	6.545	R
33-4, 98–100	399.48	103.7	46.7	63.021	150	98.4	37.4	48.390	N?
33-5, 30–32	400.30	18.5	86.8	20.698	150	135.7	−19.1	4.244	R
34-1, 131–133	404.81	271.2	6.5	6.726	150	285.1	−15.5	6.630	R
34-2, 135–137	406.35	250.9	−3.5	0.898	150	254.5	−19.9	0.528	R
34-3, 34–36	406.84	226.8	−25.7	1.254	150	227.8	−42.6	0.974	R
34-4, 16–18	408.16	181.2	−1.2	0.073	NRM				R
34-4, 28–30	409.78	141.8	−14.6	0.100	NRM				R
34-6, 13–16	411.13	320.4	−9.5	23.789	150	252.2	−35.3	23.678	R
34-6, 136–138	412.36	259.2	63.5	0.023	NRM				?
35-1, 31–33	413.31	317.6	−35.8	0.440	150	324.6	−31.5	0.426	R
35-1, 97–99	413.97	261.9	−8.9	0.237	50	26.2	6.4	0.084	R
35-4, 83–85	418.33	291.0	−25.4	0.054	NRM				R
35-5, 51–53	419.51	1.3	−17.7	0.876	50				R
36-2, 101–103	425.5	110.4	57.9	69.120	50	99.9	55.7	47.021	N
36-3, 146–148	426.96	41.1	84.6	3.969	50	168.8	42.5	0.634	N
36-4, 124–126	428.24	138.4	28.2	0.047	NRM				N
37-1, 10–12	432.10	210.7	57.7	0.261	25	211.2	70.3	0.305	N
27-2, 54–56	434.04	321.7	83.1	0.235	25	20.5	72.2	0.251	N
37-3, 42–44	435.42	126.1	−.56	0.048	NRM				R
37-3, 119–121	436.19	7.6	9.8	0.028	NRM				?
37-4, 125–127	437.75	327.6	29.5	0.039	NRM				?
37-5, 52–54	438.52	102.5	−9.5	0.017	NRM				R
38-1, 127–130	442.77	161.4	−43.3	0.490	25	187.8	−47.8	0.592	R
38-2, 28–30	443.28	305.1	46.0	0.069	NRM				N
38-3, 10–12	444.60	41.3	42.1	0.012	NRM				N
38-5, 33–35	447.83	181.7	54.0	0.105	NRM				N
38-5, 86–88	448.36	345.1	35.6	10.249	150	314.0	38.7	1.462	N
38-6, 9–11	449.09	285.3	−4.8	0.161	25	273.7	−56.3	0.145	R
38-6, 191–93	449.91	317.5	−22.3	0.429	50	329.3	−27.2	0.172	R

Table 4. (Continued).

Core-Sample (interval in cm)	Sub-bottom depth (m)	Before demagnetization D (°)	I (°)	Int (μG)	Demagnetization field (Oe)	After demagnetization D (°)	I (°)	Int (μG)	Polarity
Hole 550 (Cont.)									
39-1, 11-14	451.11	140.2	86.2	4.261	25	148.7	83.7	4.095	N
39-1, 137-140	452.37	299.1	−28.9	3.295	100	285.4	−35.9	3.075	R
39-8, 29-31	452.34	91.9	−30.1	0.074	NRM				R
39-2, 109-111	453.59	271.6	−27.4	7.931	100	274.6	−31.6	8.166	R
39-3, 134-137	455.34	248.8	−36.7	0.038	NRM				R
39-4, 6-9	455.56	24.9	−24.4	4.668	25	27.7	−22.6	4.550	R
39-5, 50-53	457.50	20.6	60.6	29.347	150	203.7	−26.3	4.622	R
39-5, 139-142	458.39	299.5	71.3	0.153	25	343.7	64.2	0.166	N
41-2, 37-39	471.87	114.0	80.4	6.613	25	100.6	84.3	6.533	N
41-2, 128-131	472.78	332.2	−74.8	78.494	150	88.2	40.3	0.869	N?
41-3, 26-29	473.26	112.1	80.4	21.80	25	127.8	77.7	17.471	N
42-1, 106-108	480.5	9.8	61.7	3.190	25	12.8	59.6	3.422	N
42-2, 45-48	481.45	87.4	63.3	0.739	25	88.2	66.9	0.878	N
43-1, 36-38	489.36	340.0	71.6	10.986	25	336.9	73.1	10.453	N
43-2, 26-28	490.76	131.8	74.0	6.728	50	133.6	78.1	6.618	N
43-3, 8-10	492.08	332.4	62.9	11.683	50	328.9	63.0	11.405	N
47-1, 20-22	522.70	294.5	67.0	30.861	50	297.2	74.7	15.132	N
47-1, 118-120	523.18	2.2	29.7	5.681	100	77.1	−42.6	4.223	R
47-2, 28-30	524.28	15.6	74.5	13.613	150	184.3	−52.1	2.737	R
47-2, 117-121	524.69	306.1	73.8	10.960	150	319.2	−24.9	0.984	R
47-3, 51-53	526.01	254.6	67.0	30.721	150	269.2	58.1	2.376	N
47-3, 105-107	526.05	162.4	67.5	12.317	150	188.4	54.8	2.025	N
Hole 550B									
1-1, 52-54	456.52	298.7	60.2	22.893	150	303.4	64.7	4.460	N
1-2, 95-97	458.45	137.3	57.5	40.250	150	157.4	46.0	21.375	N
1-3, 112-114	460.12	300.9	63.2	23.511	150	297.7	68.9	5.887	N
1-4, 128-130	461.78	136.7	78.1	27.905	300	306.0	−23.0	3.215	R
1-5, 144-146	463.44	36.6	57.1	92.584	500	330.6	−4.7	2.493	R
1-6, 9-11	463.57	246.5	63.8	73.764	400	285.4	−4.7	0.145	R
2-1, 55-57	466.05	117.4	62.8	23.865	500	9.9	35.5	0.448	?
2-1, 123-125	466.73	5.4	50.9	20.090	150	56.0	32.0	0.734	N
2-2, 99-101	467.99	344.3	74.2	58.929	500	359.3	19.0	4.513	N
2-3, 17-19	468.67	324.4	73.8	54.678	300	350.8	83.5	17.735	N
2-3, 21-24	468.71	356.5	88.5	25.564	200	330.1	−43.9	0.062	R
2-3, 32-34	468.82	305.2	43.4	25.788	200	37.8	−59.2	1.982	R
2-3, 81-83	469.31	352.7	53.3	26.096	150	159.1	−16.4	1.617	R
2-3, 113-115	469.63	68.3	80.8	25.090	150	267.1	−24.9	1.458	R
3-1, 5-6	475.05	256.5	−64.4	20.214	100	3.9	−81.7	2.235	T
3-1, 137-139	476.37	197.0	50.7	20.843	300	272.8	−66.1	0.387	R
3-2, 21-23	478.21	128.2	69.9	17.200	300	139.7	64.2	1.882	N
4-1, 26-29	484.76	193.8	68.1	8.128	300	199.9	68.1	6.810	N
4-2, 22-25	486.22	62.6	63.1	10.433	300	50.2	61.2	4.232	N
5-1, 33-36	494.33	15.9	57.5	14.469	300	14.8	52.5	3.715	N
5-2, 14-17	495.64	141.5	60.8	20.954	300	124.3	63.5	3.714	N
5-3, 10-13	497.10	257.7	58.7	5.597	300	308.0	42.2	0.807	N
5-4, 116-118	499.66	136.3	64.5	6.436	300	116.2	58.9	0.455	N
7-1, 75-77	513.75	306.3	67.6	25.483	200	333.2	72.3	4.171	N
7-2, 101-103	515.51	325.2	59.5	29.017	200	323.1	49.1	6.612	N
7-3, 42-44	518.42	119.8	65.1	34.765	200	105.9	52.4	14.195	N
8-1, 128-130	523.78	202.6	70.6	26.337	400	347.3	62.2	2.800	N
8-2, 9-11	524.00	230.3	49.3	21.742	150	220.6	39.1	2.627	N
8-2, 121-123	525.21	255.0	84.8	18.035	200	45.4	−32.2	4.677	R
8-3, 115-117	526.65	301.5	73.3	17.250	200	117.3	−53.2	0.857	R
8-3, 123-125	526.73	30.9	−74.1	22.563	NRM				R
8-3, 127-129	526.77	54.1	−66.4	23.503	200	335.4	−71.7	1.097	R
8-3, 131-133	526.81	300.5	67.5	23.152	300	106.8	44.0	0.118	N
8-3, 147-149	526.97	286.0	64.2	28.129	200	290.3	65.5	2.747	N
8-4, 11-13	527.11	307.4	66.3	25.810	200	267.6	58.8	2.823	N
8-4, 125-127	528.25	356.2	69.8	23.755	200	17.0	60.8	1.628	N
8-5, 93-95	529.43	289.8	67.6	35.543	200	306.8	65.8	5.025	N
8-6, 9-11	530.09	9.6	54.9	30.657	200	8.4	62.0	3.133	N
9-1, 42-45	532.45	131.5	66.7	23.260	300	162.0	31.5	0.800	N
9-2, 44-46	533.94	324.9	68.5	28.177	200	324.3	74.3	4.301	N
9-3, 33-35	535.85	31.4	24.5	0.126	NRM				N
9-3, 85-87	535.33	113.4	−24.7	0.216	25	78.6	10.6	0.259	?
9-4, 30-32	536.80	265.4	−14.8	0.175	25	236.1	−28.5	0.478	R
9-5, 22-24	538.22	81.1	58.7	0.311	25	145.8	3.9	0.066	R
10-1, 55-57	542.07	343.6	49.4	18.222	150	252.1	−19.5	3.419	R
10-3, 14-16	544.64	131.8	59.4	40.185	300	128.1	52.2	9.561	N
10-4, 78-80	546.78	18.2	41.4	0.478	25	5.4	3.7	0.221	?
10-4, 118-120	547.18	333.6	59.0	0.242	50	336.4	50.0	0.072	N
10-5, 67-69	548.17	352.6	−13.6	0.253	25	352.6	−27.2	0.228	R
11-1, 35-37	551.35	325.6	66.5	27.781	150	21.4	57.4	2.652	N
11-2, 25-27	552.75	26.6	74.4	1.320	50	185.6	69.0	0.460	N
11-3, 107-109	555.07	295.7	36.7	0.139	25	301.8	78.1	0.350	N
11-4, 28-30	555.78	71.1	17.4	0.303	25	14.3	−23.8	0.075	R
12-5, 32-34	560.82	202.9	61.1	0.355	50	74.4	82.4	0.042	N
12-2, 130-132	563.30	295.9	60.0	29.548	300	280.3	42.1	26.343	N
12-3, 9-11	563.59	51.3	49.5	29.756	400	42.4	33.5	1.184	N
12-4, 58-60	565.58	216.2	78.8	17.440	200	265.3	73.2	1.256	N
13-1, 19-22	570.19	11.9	51.7	21.997	300	11.4	14.9	3.867	N
13-2, 38-40	571.88	221.4	57.0	83.854	200	207.8	35.9	21.92	N
13-3, 15-17	573.15	68.9	54.2	36.158	400	79.9	33.2	4.616	N
13-4, 99-101	575.49	88.0	61.9	0.697	25	100.3	68.3	0.775	N
13-5, 65-67	576.65	211.9	32.0	0.315	25	215.1	60.6	0.342	N
13-6, 63-66	575.13	158.7	40.1	0.485	25	103.0	70.0	0.194	N
13-7, 15-17	579.15	3.0	5.8	2.270	50	27.7	21.2	0.828	N

Table 4. (Continued).

Core-Sample (interval in cm)	Sub-bottom depth (m)	Before demagnetization D (°)	Before demagnetization I (°)	Before demagnetization Int (μG)	Demagnetization field (Oe)	After demagnetization D (°)	After demagnetization I (°)	After demagnetization Int (μG)	Polarity
Hole 550B (Cont.)									
14-1, 6–8	579.56	195.5	43.1	0.602	50	194.1	42.0	0.813	N
14-2, 6–8	581.06	314.4	36.6	0.666	50	301.1	32.1	0.834	N
14-3, 12–14	582.62	212.6	42.7	0.545	50	198.0	49.2	0.739	N
14-4, 16–18	584.16	48.1	18.3	1.146	150	47.7	9.3	0.853	R
14-4, 126–128	585.26	45.6	−14.1	0.168	NRM				R
14-5, 41–43	585.91	331.4	−18.7	0.273	100	275.0	−21.7	0.350	R
14-5, 128–130	586.78	358.5	47.2	0.119	NRM				N
15-1, 51–53	589.51	120.6	14.0	0.228	100	146.5	36.1	0.126	N
15-1, 133–136	590.33	164.7	13.1	0.073	NRM				N
15-2, 104–107	591.54	90.9	47.3	0.799	50	89.1	51.0	0.880	N
15-3, 16–19	592.16	315.6	38.2	0.597	50	261.8	34.6	0.571	N
15-4, 119–122	594.69	173.3	40.4	0.581	50	176.4	40.5	0.387	N
15-5, 9–12	595.09	269.1	23.8	0.421	50	242.0	30.5	0.265	N
15-6, 21–24	596.71	164.2	53.1	0.306	50	203.7	32.0	0.296	N
16-1, 14–16	598.64	121.5	−24.5	0.253	50	14.3	13.7	0.439	N
16-2, 72–74	599.72	92.6	15.3	0.347	50	89.0	30.1	0.405	N
16-3, 8–10	601.58	298.7	38.0	0.349	50	344.3	12.2	0.363	N
17-1, 11–13	608.11	225.6	25.2	0.163	25	198.1	49.8	0.204	N
17-1, 116–118	609.16	205.1	58.5	0.149	NRM				N
17-2, 35–37	609.85	142.4	35.0	0.194	25	75.5	−6.5	0.315	R
17-2, 112–114	610.62	320.1	55.0	0.113	NRM				N
17-3, 26–28	611.26	157.6	25.5	0.320	25	182.9	51.3	0.287	N
17-4, 58–60	613.08	343.2	83.6	0.195	25	182.5	50.4	0.328	N
17-5, 18–20	614.18	41.1	53.6	0.217	25	163.4	48.3	0.574	N
18-1, 57–59	617.57	129.3	44.8	0.175	25	144.3	75.3	0.252	N
18-2, 59–61	619.07	303.4	50.8	0.221	25	293.6	31.7	0.147	N
18-3, 92–94	620.92	139.0	61.7	60.619	25	144.0	60.8	54.013	N
18-4, 54–56	622.04	312.3	53.4	32.996	150	314.1	42.4	7.592	N
19-4, 16–18	634.86	178.3	62.7	1.872	50	203.6	51.7	0.782	N
20-1, 31–33	635.31	284.5	63.7	74.019	100	259.3	48.8	19.746	N
20-2, 59–60	637.09	292.0	48.6	0.285	50	269.4	41.9	0.303	N
20-4, 25–26	639.75	13.1	50.2	14.291	50	16.1	48.2	10.490	N
20-5, 52–54	641.52	81.2	53.9	1.722	50	80.2	58.3	1.350	N
27-1, 124–127	645.25	243.7	57.4	1.107	NRM				N
21-2, 34–37	645.84	127.1	53.3	4.880	50	128.2	46.7	4.899	N
21-3, 22–25	647.22	290.7	51.6	2.560	50	284.2	52.3	2.221	N
21-4, 31–34	648.81	235.4	55.3	2.431	50	245.4	41.2	2.193	N
21-6, 27–30	651.77	293.3	46.8	5.614	50	294.6	48.8	5.280	N
22-1, 28–31	653.28	318.2	59.0	3.409	50	80.2	58.3	1.350	N
22-1, 121–123	654.21	132.4	39.4	0.553	50	266.1	43.0	0.649	N
22-2, 33–35	654.83	244.5	42.9	0.783	50	266.1	43.0	0.649	N
22-2, 107–109	655.57	263.4	40.0	1.458	50	255.6	49.5	1.766	N
22-3, 20–23	656.20	263.2	60.9	7.952	50	267.1	51.5	4.711	N
22-3, 99–101	656.99	202.5	48.2	4.362	100	197.7	47.8	4.383	N
22-5, 38–40	659.38	163.8	41.1	5.018	50	166.7	44.7	5.494	N
22-5, 107–116	660.07	352.6	52.8	13.136	100	327.8	55.7	5.707	N
22-6, 7–10	660.57	291.0	40.7	3.430	50	284.9	32.1	2.084	N
22-6, 135–140	661.88	20.1	44.8	1.857	100	16.7	44.5	2.244	N
23-1, 8–10	662.08	236.9	54.1	31.172	150	223.1	37.7	9.007	N
23-1, 105–108	663.05	274.4	−85.3	101.46	50	193.4	−88.4	53.134	R
23-2, 14–17	663.44	0.2	50.8	30.805	150	9.5	44.1	7.406	N
23-2, 92–94	664.42	48.5	55.7	16.779	50	19.6	49.4	11.094	N
23-3, 89–92	665.89	261.1	−57.6	39.136	50	254.9	−53.4	27.732	R
24-1, 91–93	671.91	102.3	60.5	101.733	50	112.7	58.5	61.812	N
24-2, 88–90	673.38	54.2	45.7	125.303	150	53.8	30.2	24.880	N
24-3, 38–40	674.38	210.0	52.9	120.167	800	274.6	11.0	3.469	N
25-1, 29–31	680.29	48.2	45.6	162.950	200	49.7	33.0	23.778	N
25-2, 122–125	682.72	49.1	45.2	263.152	500	332.2	−4.0	6.816	R
25-3, 27–29	683.27	291.3	42.5	236.584	500	350.4	45.0	3.664	N
25-1, 49–51		297.5	49.1	1217.50	NRM				
29-1, 81–83		268.9	56.8	1638.13	NRM				

Note: Symbols and abbreviations as in Table 1.

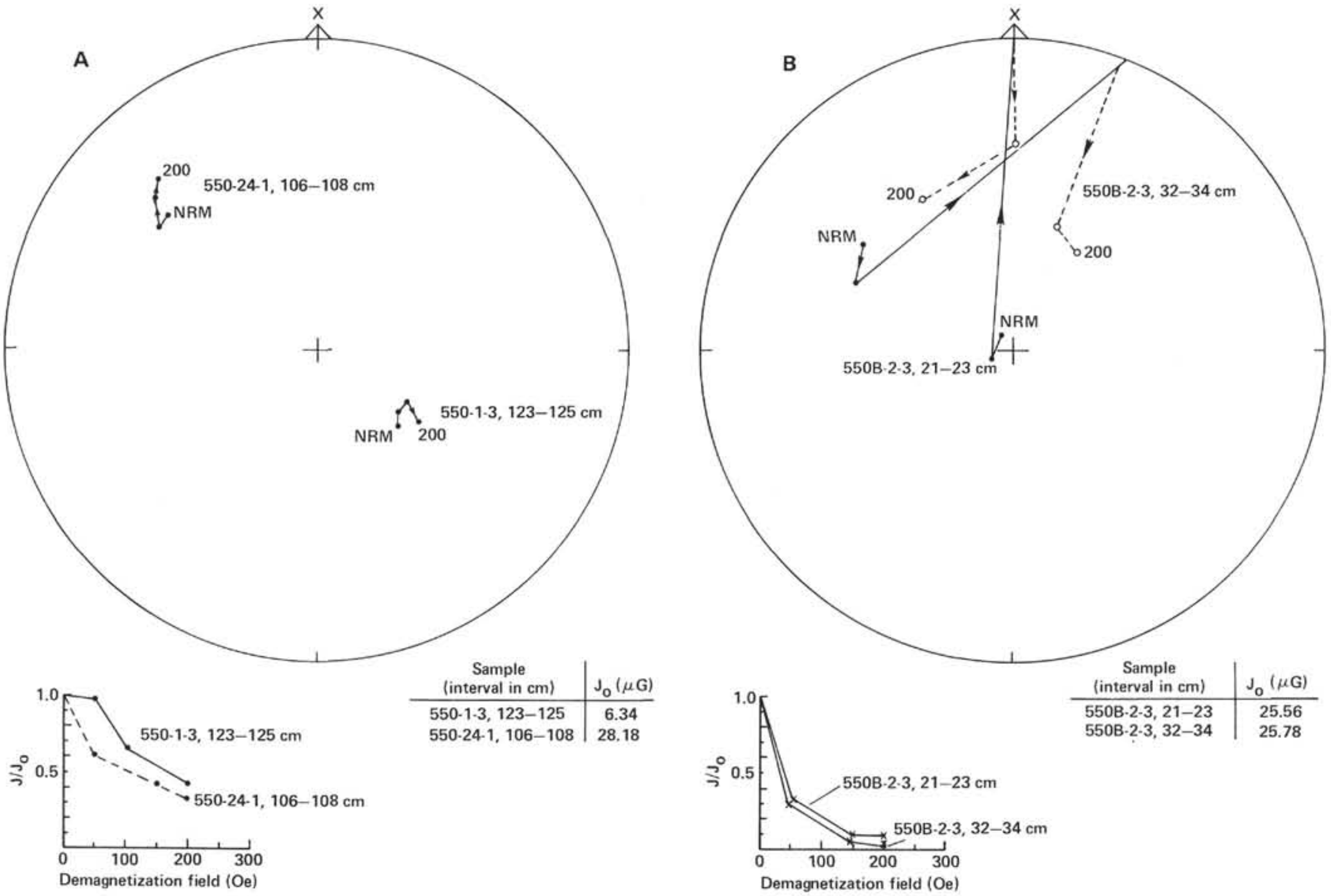

Figure 15. The response of representative samples from Site 550 to af demagnetization. A. Samples from Hole 550. B. Samples from Hole 550B. Symbols as in Fig. 2.

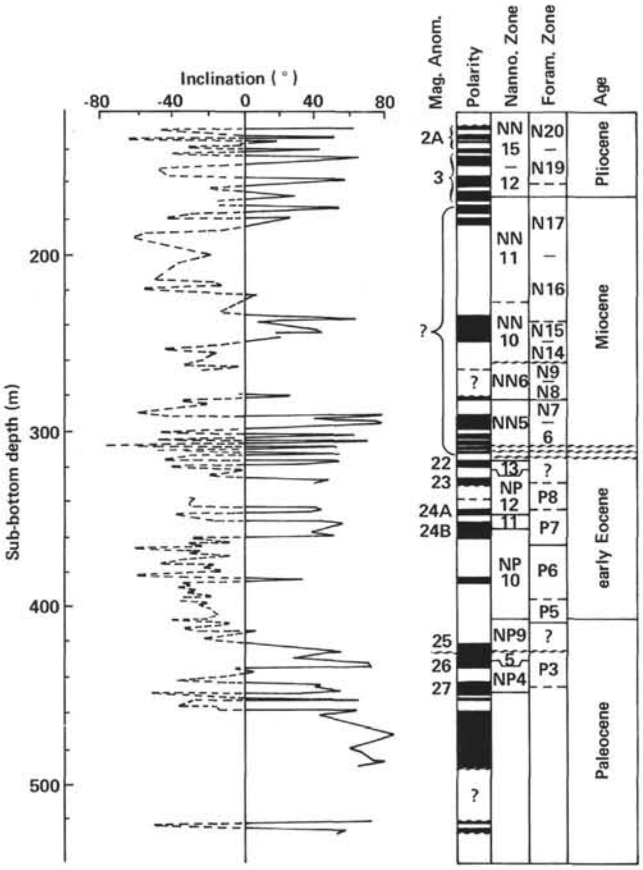

Figure 16. Downhole variation of magnetic inclination and the inferred polarity reversal sequence for Hole 550.

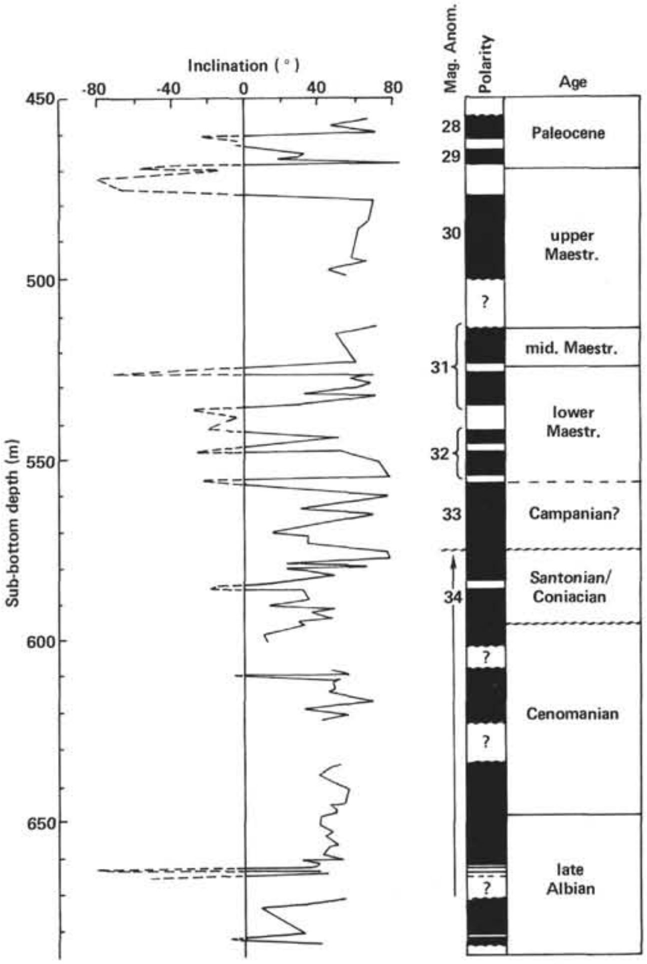

Figure 17. Downhole variation of magnetic inclination and the inferred polarity reversal sequence for Hole 550B.

Table 5. Paleomagnetic results, Hole 551.

Core-Section (interval in cm)	Sub-bottom depth (m)	Before demagnetization D (°)	Before demagnetization I (°)	Before demagnetization Int (μG)	Demagnetization field (Oe)	After demagnetization D (°)	After demagnetization I (°)	After demagnetization Int (μG)	Polarity
2-2, 27-29	105.77	323.3	37.0	7.941	500	300.9	−8.2	0.519	R
2-3, 92-94	107.92	109.0	68.8	9.702	300	131.3	40.0	1.341	N
3-1, 56-58	114.06	320.3	41.4	9.219	500	321.3	4.7	0.274	R?
3-2, 31-34	115.31	155.0	54.6	10.64	500	210.9	−1.9	0.518	R
3-3, 24-26	116.74	15.3	80.6	15.39	500	346.1	51.6	0.703	N
4-1, 44-46	123.44	16.1	45.8	20.96	300	42.0	18.3	0.549	?
4-2, 83-85	125.33	28.7	30.1	11.90	300	339.7	24.2	0.395	N
4-3, 89-91	126.89	218.2	62.7	16.697	300	227.5	20.0	1.630	N
4-4, 80-82	128.30	317.5	45.4	17.8	600	287.4	28.5	0.94	N
5-1, 20-22	132.70	54.3	72.6	2.93	100	310.6	−34.9	0.59	R
5-2, 27-29	134.27	38.4	−1.8	0.30	75	22.3	−8.9	0.207	R
5-2, 58-61	139.08	286.5	80.2	0.41	75	196.7	62.6	0.18	N
6-2, 141-143	141.41	257.5	37.7	0.97	100	266.5	37.4	0.47	N
6-3, 72-75	142.22	140.7	−16.6	4.179	100	112.9	−63.2	14.70	R

Note: Symbols and abbreviations as in Table 1.

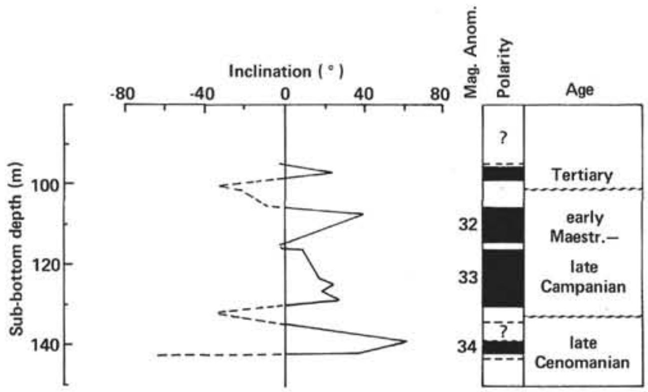

Figure 18. Downhole variation of magnetic inclination and the inferred polarity reversal sequence, Site 551.

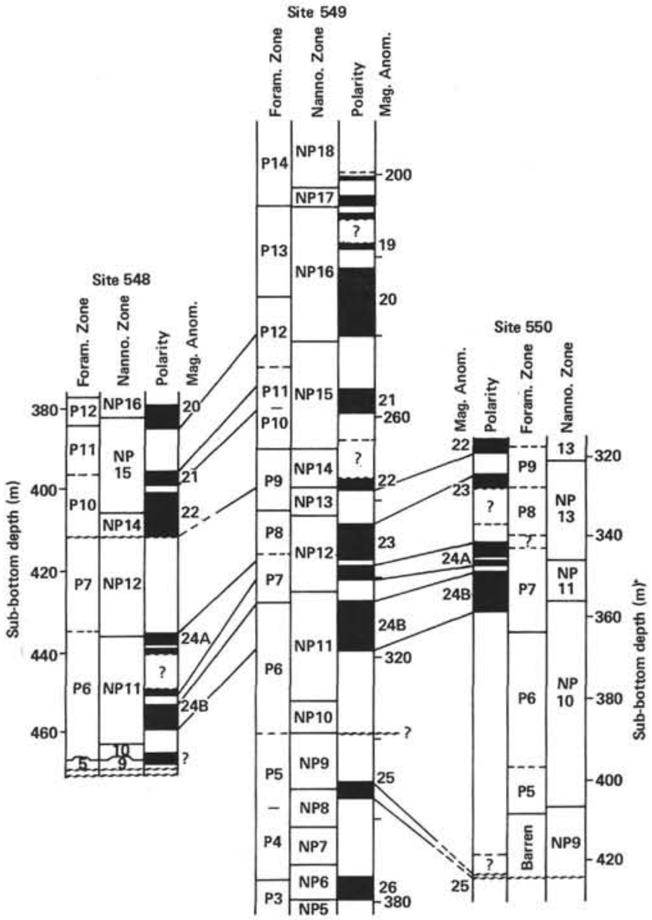

Figure 19. Magnetostratigraphic correlation of the middle Eocene to upper Paleocene sediments from Sites 548, 549, and 550.